



## Strategies for Optical Trapping in Biological Samples: Aiming at Microrobotic Surgeons

**Bunea, Ada-Ioana; Glückstad, Jesper**

*Published in:*  
Laser & Photonics Reviews

*Link to article, DOI:*  
[10.1002/lpor.201800227](https://doi.org/10.1002/lpor.201800227)

*Publication date:*  
2019

*Document Version*  
Peer reviewed version

[Link back to DTU Orbit](#)

*Citation (APA):*  
Bunea, A-I., & Glückstad, J. (2019). Strategies for Optical Trapping in Biological Samples: Aiming at Microrobotic Surgeons. *Laser & Photonics Reviews*, [1800227]. <https://doi.org/10.1002/lpor.201800227>

---

### General rights

Copyright and moral rights for the publications made accessible in the public portal are retained by the authors and/or other copyright owners and it is a condition of accessing publications that users recognise and abide by the legal requirements associated with these rights.

- Users may download and print one copy of any publication from the public portal for the purpose of private study or research.
- You may not further distribute the material or use it for any profit-making activity or commercial gain
- You may freely distribute the URL identifying the publication in the public portal

If you believe that this document breaches copyright please contact us providing details, and we will remove access to the work immediately and investigate your claim.

**Article type:** Review

## **Strategies for optical trapping in biological samples: Aiming at microrobotic surgeons**

*Ada-Ioana Bunea\**, *Jesper Glückstad*

Dr. A.-I. Bunea, Prof. J. Glückstad  
DTU Fotonik, Dept. of Photonics Engineering, DK-2800 Lyngby, Denmark  
\*adabu@dtu.dk

**Keywords:** optical trapping, optical manipulation, beam-shaping, Light Robotics, microrobots

Optical trapping and manipulation of objects down to the Ångstrom level has revolutionized research at the smallest scales in all natural sciences. The flexibility of optical trapping methods facilitates real-time monitoring of the dynamics of biological processes in model systems and even in living cells. Different optical trapping and manipulation approaches allow displacement of nanostructures with subnanometer precision and force measurements with femtonewton precision. Due to inherent constraints of optical methods, most optical trapping experiments are performed in water or simple aqueous solutions. However, in recent years, there is an ever-growing interest of shifting from simple aqueous media towards more biologically-relevant media. Precise optical trapping and manipulation, combined with state-of-the-art microfabrication, would enable the development of microrobotic “surgeons” with tremendous potential for biomedical and microengineering applications. This review will introduce the basics of optical trapping and discuss its applications for biological samples, with focus on trapping in biological media and strategies for overcoming the challenges of optical manipulation in complex environments as a stepping-stone for microrobotic “surgeons”.

### **1. Introduction**

Almost half a century has passed since the first demonstration of optical manipulation from Arthur Ashkin.<sup>[1]</sup> 1986 brought the first publication on “a single-beam gradient force radiation-pressure particle trap”,<sup>[2]</sup> a technique which later rose to glory under the name of “optical tweezers” and brought Ashkin ½ of the Nobel Prize in Physics 2018 "for the optical tweezers and their application to biological systems."

Ever since its original demonstration, optical trapping has continuously evolved and helped revolutionize research by providing unprecedented micromanipulation possibilities. Optical trapping provides non-contact, non-destructive and precise manipulation of micro- and nanometer sized objects. The applications of optical trapping span all fields of natural sciences, from cellular manipulation and characterization of biological systems to micro- and nanopatterning or plasmonic applications. A hybrid technique, magneto-optical trapping, is employed for confining and cooling atoms.<sup>[3,4]</sup>

Early optical trapping experiments were performed on transparent microspheres. As the field evolved, the range of trapped objects expanded to include various types of micro- and nano objects. The development of optically-controlled microfabricated tools with embedded functionalities has led to the emergence of a new research field, Light Robotics.<sup>[5]</sup> In Light Robotics, intelligent beam sculpting is employed for actuating microrobots designed for specific applications at the microscale. In order for Light Robotics to achieve its full potential, we believe that the microrobots need to perform well in biological samples.

This review paper aims at discussing the state of the art and the future of optical trapping in biological samples. We start by explaining the basic concepts of optical trapping and beam-shaping and we present different ways to generate single and multiple traps. We then briefly mention the current applications of optical trapping in aqueous solutions and expand on the applications in complex media. Finally, we discuss strategies for improving optical trapping

in biological samples, and how these can help further the field of Light Robotics towards the development of microrobotic “surgeons”.

## 2. Basic concepts of optical trapping

Optical trapping relies on exploiting light-matter interactions (**Figure 1**). The basic principles behind optical trapping and its applications have been reviewed by numerous groups throughout the years.<sup>[6–14]</sup> Briefly, two different types of forces are involved: gradient forces, which pull the object towards the laser beam’s focal point, and scattering forces, which push the object along the direction of the laser beam propagation. Other factors, such as Stokes’ drag force and Brownian motion, also contribute to the stability of the trap.<sup>[13,15]</sup> A short description of the physics of optical trapping for isotropic and anisotropic particles is provided in the following sections.

### 2.1. Trapping spherical particles

For isotropic homogeneous spheres, the Lorenz-Mie theory describes electromagnetic scattering upon plane wave illumination.<sup>[12]</sup> For this type of particles, light–matter interactions can be classified based on the relation between particle size and wavelength as being:

*i)* In the *geometric optics regime*, where the particle diameter is an order of magnitude larger than the laser wavelength, the reflection and refraction of light generate gradient forces pulling the particle towards the beam focus (**Figure 1B** and **1C**) and scattering forces that tend to destabilize the trap. Briefly, consider a transparent, spherical particle in a light field characterized by inhomogeneous intensity distribution in a plane transverse to the optical axis. A light ray of power  $P$  travelling in a medium with a refractive index  $n_{med}$  is associated with a linear momentum flux  $\mathbf{p} = n_{med}P/c$ . The vector sum of the momentum flux for a spherical particle that is not at equilibrium within the light field will point away from the region of highest intensity, causing the sphere to experience a gradient force  $\mathbf{F}_{grad}$  along the intensity gradient (Figure 1B).<sup>[2]</sup> A scattering force  $\mathbf{F}_{scat}$  accompanies the gradient force along the

optical axis. The scattering force is enhanced by reflection and absorption. When the balance of forces is in favor of the gradient forces, the object can be stably trapped in the light focal point, as shown in Figure 1 for simple gradient force optical tweezers. In this case, the refractive index difference between the particle and the trapping media will largely influence the trap stability.

ii) In the *Rayleigh regime*, where the particle is an order of magnitude smaller than the wavelength. Here, the electric field of the light induces a dipole in the particles. The polarized particle minimizes its energy and is therefore most stable in the beam focal point due to the high field gradients present. In the Rayleigh regime, the trap stability is largely influenced by the particle polarizability. The theoretical expressions of the forces exerted by radiation on a dielectric sphere in the Rayleigh regime were reported by Harada and Asakura.<sup>[16]</sup>

The Rayleigh approximation considers the dielectric particle a volume of infinitesimal point dipoles which interact with the electromagnetic field of the light.<sup>[15-17]</sup> The induced dipole moment  $\vec{p}_d$  of a sphere of radius  $r$  in a homogeneous electric field  $\vec{E}$  can be written as:<sup>[16]</sup>

$$\vec{p}_d = 4\pi n_{med}^2 \epsilon_0 r^3 \left( \frac{m^2 - 1}{m^2 + 2} \right) \vec{E} \quad (1)$$

where  $\epsilon_0$  is the vacuum permittivity,  $\epsilon_0 = 8.85 \text{ pF} \cdot \text{m}^{-1}$ , and  $m$  is the relative refractive index of the particle,  $m = n_{part}/n_{med}$ .

Thus, the particle will experience a gradient force due to the Lorentz force acting on the dipole induced by the electromagnetic field,  $\vec{F}_{grad}$ .<sup>[16]</sup>

$$\vec{F}_{grad} = \pi n_{med}^2 \epsilon_0 r^3 \left( \frac{m^2 - 1}{m^2 + 2} \right) \nabla |\vec{E}|^2 = \frac{2\pi n_{med} r^3}{c} \left( \frac{m^2 - 1}{m^2 + 2} \right) \nabla I \quad (2)$$

where  $I$  is the irradiance.

The scattering force  $\vec{F}_{scat}$  is caused by the harmonic oscillations of the electric field in time and, for an incident Gaussian beam, it can be written as:<sup>[16]</sup>

$$\vec{F}_{scat} = \frac{8\pi n_{med} k^4 r^6}{3c} \left( \frac{m^2 - 1}{m^2 + 2} \right) \vec{I} \quad (3)$$

where  $k$  is the wavenumber of the trapping beam,  $k = 2\pi/\lambda$ .

The gradient force is a conservative force and is the gradient of a scalar function, the trapping potential, which can be written as:<sup>[15]</sup>

$$U = \frac{2\pi n_{med} r^3}{c} \left( \frac{m^2 - 1}{m^2 + 2} \right) I \quad (4)$$

Trapped particles are subject to thermal fluctuations and thus undergo Brownian motion, which works towards destabilizing the trap. Viscous drag dampens the effect of Brownian motion and thus contributes to stabilizing the trap. The thermal kinetic energy of a particle in the optical trap is  $k_B T$ , where  $k_B$  is the Boltzmann constant and  $T$  is the absolute temperature.<sup>[15]</sup> If the trapping potential  $U$  is significantly higher than  $k_B T$ , the particle is not likely to escape the trap due to Brownian motion.

*iii) In the intermediate regime*, where the particle is of similar size to the laser wavelength.

This is the most common case for optical trapping experiments. Here, the behavior of the particle in relation to light is intermediary to the geometric optics and Rayleigh regimes and can be modelled through the generalized Lorenz-Mie theories.<sup>[18,19]</sup>

The scattering of a linearly polarized electromagnetic plane wave by a homogeneous sphere is described by the equations of the Lorenz–Mie theory (LMT). Lasers, however, emit transversely localized beams, therefore the LMT cannot be applied as such for describing the scattering of a laser beam by a particle.<sup>[20]</sup> This led to the development of the generalized Lorenz–Mie theories (GLMT), which describe the scattering of electromagnetic arbitrary shaped beams by a homogeneous sphere. The mathematical description of the beam illuminating the sphere is one of the most challenging elements in the GLMT. Most approaches use either an analytic approximation of the beam fields, or express the fields in terms of an infinite series of spherical multipole partial waves with specified coefficients.<sup>[20]</sup>

The calculation of optical forces in the intermediate regime is the subject of intense research<sup>[12,20–23]</sup> and will not be further detailed in this review.

## 2.2. Trapping anisotropic particles

Optical trapping was first demonstrated on transparent latex microspheres.<sup>[1]</sup> A variety of applications for microsphere trapping have since been reported and the theory behind spherical object trapping has been thoroughly investigated. Many microscopic objects of interest, such as bacteria, mammalian cells, carbon nanotubes etc. are non-spherical particles, and these can also be optically trapped and manipulated.<sup>[24–27]</sup> Naturally, it is more difficult to model and calculate the forces for non-spherical particles, which is why computational models have been developed.<sup>[28,29]</sup> Theoretical calculation and experimental measurement of optical forces on non-spherical particles has been reported by several groups.<sup>[30–38]</sup>

A review on trapping of nanostructures covering non-spherical particles, such as nanowires and carbon nanotubes, was published in 2013 by Maragò *et al.*<sup>[39]</sup> S. H. Simpson has recently reviewed the optical trapping of anisotropic particles, covering a variety of particle shapes, including microtools, and optically anisotropic particles.<sup>[40]</sup> The theories and approximations for calculating forces and torques on anisotropic particles are discussed in more details in Simpson's review.<sup>[40]</sup>

## 2.3. Laser light propagation modes

Laser sources commonly have a Gaussian beam profile, meaning that the intensity distribution in all planes perpendicular to the beam propagation axis can be described with a Gaussian function, and the width of the Gaussian intensity profile changes along the axis.<sup>[41]</sup> A Gaussian beam narrows to its minimum diameter at the beam waist, which is characterized by a planar phase front.

Conventional optical tweezers are often performed using Gaussian beams. However, some of the more recent optical trapping methods employ advanced beam-shaping to improve

trapping. The theory and applications of beam-shaping techniques are discussed in more detail in recent review papers,<sup>[42–44]</sup> Roadmap on structured light,<sup>[45]</sup> and Dickey's book on laser beam-shaping.<sup>[46]</sup> Beam-shaping is a field in itself and will only be discussed briefly as part of this review paper.

Beam-shaping can be achieved with the use of diffractive optical elements,<sup>[47,48]</sup> which are usually placed in the Fourier plane conjugate with the back aperture objective. Axicons,<sup>[49]</sup> microfabricated diffractive optical elements, are widely used for beam-shaping. Alternatively, holographic methods, typically based on the use of a spatial light modulator (SLM), can provide flexible beam-shaping when combined with the proper algorithms.<sup>[50]</sup> SLMs are commonly used as phase-only beam-shaping devices, since amplitude modulation can decrease the available optical power.<sup>[51]</sup> Some examples of elaborate laser modes – Bessel, Airy and Laguerre-Gaussian beams – generated with the aid of diffractive elements are shown in **Figure 2**.<sup>[51]</sup> Shaping a Gaussian beam into two stripe-like elongated beams with opposite transverse momenta was recently used to generate “tug-of-war” tweezers.<sup>[52]</sup> An optical Archimedes' screw was recently reported by Hadad *et al.*<sup>[53]</sup> An optical twister, a diffracting beam with a spiral profile on both the amplitude and phase of the beam, was reported by our group.<sup>[54]</sup> Furthermore, our group has pioneered Generalized Phase Contrast (GPC), a phase-only beam-shaping method, in the '90s.<sup>[55–57]</sup> The theory and applications of GPC are described in the book by Glückstad and Palima<sup>[58]</sup> and the forces involved in GPC-based optical trapping are discussed in Rodrigo *et al.*<sup>[59]</sup> More recently, a hybrid method between holography and GPC, Holo-GPC, was developed.<sup>[60]</sup> Holo-GPC combines the advantages of GPC and holography and can be used for generating well-defined, speckle-free light shaping with extended 3D volume distribution.

#### **2.4. Approaches for generating single and multiple optical traps**

The first optical trap was reported in 1970 by Arthur Ashkin and was based on two counterpropagating, coaxially aligned beams.<sup>[1]</sup> Ashkin's groundbreaking paper described two other potential designs for optical trapping: *i*) single-beam gradient force traps, now commonly known as optical tweezers, which Ashkin first demonstrated 16 years later.<sup>[2]</sup> The forces involved in trapping with optical tweezers are discussed in detail by Ashkin.<sup>[61]</sup> *ii*) bottle beam traps, which gathered a lot of interest in the beginning of the 21<sup>st</sup> century.<sup>[62–64]</sup> Examples of how to generate multiple bottle beams traps are shown in McGloin *et al.*<sup>[65]</sup> and Alpmann *et al.*<sup>[66]</sup>

As a natural continuation to single-trap optical manipulation, the interest for generating multiple optical traps came in the early '90s. Burns *et al.* reported the generation of a large number of optical traps by using interference.<sup>[67]</sup> Masuhara's group in Japan was among the first to demonstrate double-beam laser manipulation by splitting a circularly polarized laser beam into horizontally and vertically polarized laser beams with the aid of a polarizing beam splitter.<sup>[68]</sup> This facilitated independent manipulation of two particles simultaneously. A multiple trap manipulator based on rapid sequential illumination of different points in a sample was demonstrated by Visscher *et al.*<sup>[69]</sup> Currently, a number of different techniques are commonly employed for generating single or multiple optical traps. The most widely used are discussed below and some examples are shown in **Figure 3**.

#### 2.4.1. Optical trapping using counterpropagating beams

Different optical trapping methods based on counterpropagating beams have been reported since Ashkin's initial approach. **Figure 3A** shows a schematic of a counterpropagating beam optical trap.<sup>[70]</sup> Lyons and Sonek developed a dual fiber trap system based on two coaxial optical fibers coupled to 1310 nm 20 mW cw diode lasers.<sup>[71]</sup> In their system, a microbead positioned in between the two optical fibers could be displaced over several hundred micrometers on the dual fiber axis by adjusting the relative optical power levels between the

fibers. A system based on two non-coaxial optical fibers was reported by Taguchi *et al.* and employed for lifting microspheres from the bottom of a container.<sup>[72]</sup> The trapping forces for counterpropagating dual-beam and for multiple beam fiber optic traps are discussed by Sidick *et al.*<sup>[73]</sup> Ebert *et al.* characterized the thermal properties of a dual-beam trap in a microfluidic channel.<sup>[74]</sup> A trap constructed by Shvedov *et al.* using two Laguerre-Gaussian counterpropagating and co-rotating vortex beams was employed for manipulating microscopic particles over millimeter distances and is shown schematically in **Figure 3B**.<sup>[75]</sup> A holographic system able to switch between Gaussian, Bessel and Laguerre-Gaussian modes was reported by Čižmár *et al.*<sup>[76]</sup> Holographic twin traps accommodating a long working distance were reported by Zwick *et al.*<sup>[77]</sup> An optical mirror trap was constructed by Pitzek *et al.* by shaping two collinear beams with an SLM to form a predefined focus each, one before a planar mirror and one after reflection off the mirror, in a system utilizing low NA objectives and thus offering a large field of view.<sup>[78]</sup> Our group's proprietary GPC technique is one of the earliest that utilizes low NA objectives and thus offers a large field of view. Simultaneous manipulation of high- and low-index particles and/or cells based on counterpropagating GPC-shaped beams was demonstrated.<sup>[79–82]</sup>

#### 2.4.2. Holographic optical tweezers

A collimated laser beam can be shaped with the aid of a diffractive beamsplitter, transferred to the back aperture of an objective lens and focused into a trapping array.<sup>[83,84]</sup> By using a computer-generated hologram as diffractive beamsplitter, holographic optical tweezers (HOTs) are obtained.<sup>[83]</sup> To avoid loss of power due to beam amplitude modulation's subtractive approach, the use of phase-only holograms is preferred.<sup>[84]</sup> A schematic of a HOT setup is shown in **Figure 3C**.<sup>[85]</sup> The theory for calculating forces and torques in holographic optical trapping is detailed in Sun *et al.*<sup>[86]</sup> HOTs allow simultaneous manipulation of a relatively large number of particles and are therefore particularly useful for nanopatterning

and nanofabrication.<sup>[87,88]</sup> Ideally, hologram generation for HOTs should be rapid and its customization should be user-friendly.<sup>[89]</sup> HOTs and their applications in lab-on-chip devices was reviewed by Padgett and Di Leonardo.<sup>[90]</sup>

#### 2.4.3. Dark optical traps

To manipulate low-index particles and to minimize the risk of photodamage, different methods to generate single dark optical traps were developed. Sasaki *et al.* demonstrated trapping of metal particles and water droplets by rapidly scanning the laser beam focus in circular loci around the target particles with repetition rates of 25-50 Hz.<sup>[91]</sup> He *et al.* employed Laguerre-Gaussian higher-order doughnut beams for generating dark optical traps.<sup>[92]</sup> Gahagan and Swartzlander Jr. reported trapping of particles in the dark central core of a Gaussian beam containing an optical vortex shown in **Figure 3D**.<sup>[93]</sup> Both the doughnut beams and the optical vortex beams were obtained with the aid of digital holography. As an alternative, a two-dimensional interferometric dark optical trap was reported by MacDonald *et al.*<sup>[94]</sup> Dynamic arrays of independently-configurable dark optical traps were reported by Daria *et al.* and were generated by spatial phase filtering of a phase-encoded incident light source at the Fourier plane of a 4f lens imaging system.<sup>[95]</sup>

#### 2.4.4. Plasmonic tweezers

Conventional optical tweezers suffer from severe limitations for trapping in the Rayleigh regime for particles between 1 and 100 nm, a size range in which thermal fluctuations tend to overcome the trapping forces that arise from electric dipole interactions.<sup>[39,96,97]</sup> Optical trapping of nanostructures, such as metal nanoparticles, plasmonic nanoparticles, quantum dots, carbon nanotubes, etc., was recently reviewed by Maragò *et al.*<sup>[39]</sup> A review paper from Lehmuskero *et al.* focused on the optical trapping of metal nanoparticles.<sup>[98]</sup>

To achieve stable trapping and manipulation of nanometer-sized objects, plasmon nano-optics is one of the most efficient methods. Plasmon-assisted optical trapping can refer either to the

trapping of nanoparticles that have plasmonic properties,<sup>[99]</sup> or, more commonly, to the use of plasmonic landscapes for trapping dielectric particles. Surface plasmon-assisted microtrapping was reviewed by several groups<sup>[96,100–102]</sup> and its principles and applications are explained in Urban *et al.*<sup>[103]</sup> Plasmonic tweezers use evanescent fields for optical trapping, as illustrated in **Figure 3E**.<sup>[102]</sup> The surface plasmons present at metal/dielectric interfaces can facilitate stable trapping of nanometer-sized particles even while using non-focused illumination with intensities considerably lower than those employed by conventional optical tweezers.<sup>[104]</sup> Illuminating a homogeneous gold surface by an asymmetrical non-focused laser beam generated a homogeneous in-plane optical potential which does not enable trapping. However, when using a patterned gold surface containing nanoapertures<sup>[105,106]</sup> or sharp features,<sup>[107,108]</sup> stable trapping wells can be generated due to the in-plane intensity gradients formed around the metal structures. Double nanohole plasmonic trapping has been employed for trapping single proteins and nanometer sized particles.<sup>[109–111]</sup> Various nanostructures have been employed for plasmon-assisted optical trapping, such as plasmonic nanoblock pairs<sup>[112]</sup> and arrays of nanodots, nanodiscs or nanopillars,<sup>[104,113]</sup> nanoantennas,<sup>[114]</sup> diabolical nanoantennas,<sup>[115]</sup> dipole antennas,<sup>[116]</sup> bowtie nanoantennas,<sup>[117]</sup> or gold nanodimers.<sup>[118]</sup>

### 3. Applications for biological samples

Presently, optical trapping is employed as a tool for a wide range of experiments of biological relevance. Some of the biological applications of optical trapping methods were reviewed by Fazal and Block<sup>[119]</sup> and by Villangca *et al.*<sup>[120]</sup> Optical trapping for biosensing was recently reviewed by Rodríguez-Sevilla *et al.*<sup>[121]</sup> The most widespread applications of optical trapping in biology are briefly discussed in the following sections and shown schematically in **Figure**

#### 4.

##### 3.1. Single molecule studies

Optical tweezers are among the most employed tools for single molecule studies, particularly for investigating the conformational dynamics of proteins and nucleic acids.<sup>[109,122–124]</sup>

Using stand-alone techniques, or combining fluorescence, mechanics, electrical and *in silico* methods has allowed scientists to increase the spatio-temporal resolution and the complexity of single-molecule measurements.<sup>[125,126]</sup>

Ångstrom-level resolution was first reported in 2005 by Abbondazieri *et al.*<sup>[127]</sup> through the development of an ultra-stable dual-trap configuration system. This enabled then to monitor the movement of RNA polymerase during transcription at single base pair resolution. A schematic of the system is shown in **Figure 4A**.

Dieterich *et al.*<sup>[128]</sup> used highly stable miniaturized laser tweezers based on counter-propagating laser beams for measuring the (un)folding of DNA molecules in DNA hairpin systems of different lengths. This facilitated the measurement of non-equilibrium temperatures at single molecule level under stochastically driven non-equilibrium steady states. The forces and displacements of optically trapped beads were measured with a resolution of 0.1 pN and 1 nm at 1 kHz rate.

### 3.2. Raman analysis

“Raman tweezers”, the combination of optical trapping and Raman analysis, has been widely applied for characterizing various micrometer-sized particles, such as aerosols, gas bubbles, polymorphs and living cells.<sup>[129]</sup> Optical trapping of a particle for an extended period of time (generally on the order of tens of seconds) allows acquiring a Raman spectrum, which provides information about the chemical composition of the particle. In most cases, a single laser is used for both trapping the particle of interest and for sample excitation.<sup>[129]</sup> A schematic representation of Raman tweezers is shown in **Figure 4B**.

Conventional Raman tweezers are generally not very effective for analyzing individual nanoparticles. This is mainly due to the fact that the gradient force that should ensure optical

trapping is too weak and thus often unable to overcome destabilizing effects by Brownian motion and scattering forces.<sup>[130]</sup> In recent years, a number of publications have proposed different approaches for enhancing the trapping stability and applying Raman tweezers to nanoparticles. Improved trapping of micro- and nanoparticles was reported in counterpropagating dual beam optical traps.<sup>[131,132]</sup> By using a standing wave optical trap combined with confocal Raman spectroscopy, Wu *et al.* demonstrated stable trapping of nanoparticles and a 4-8 fold increase in Raman signal.<sup>[130]</sup>

Metal particles are rather difficult to manipulate using optical forces due to their reflectivity. Successful optical manipulation of gold nanoparticles was reported as early as 1994<sup>[133]</sup> and since then a range of metal particles have been optically trapped.<sup>[98,134,135]</sup> In addition to plasmonic applications, metal nanoparticles are particularly interesting for surface enhanced Raman scattering (SERS), which was first discovered in 1974 and correctly interpreted in 1977.<sup>[136]</sup> Briefly, SERS can provide amplification of the Raman signal of the analyte molecules as a consequence of plasmon resonance excitations cause by the interaction of light with metals. SERS requires the analyte molecules to be on the surface of the metal, or in its immediate proximity, at a distance below 10 nm. Furthermore, stronger SERS signals can be acquired from closely spaced metal nanoparticles compared to single nanoparticles.<sup>[137]</sup> Thus, there has been significant interest in overcoming the challenges of trapping metal nanoparticles for harnessing the SERS effect in Raman tweezers. One successful approach is trapping with a laser with a frequency significantly different from the localized surface plasmon resonance.<sup>[137,138]</sup> In another approach, transparent particles can be metalized to create optically trappable SERS probes.<sup>[139,140]</sup> Reversible aggregation of metallic nanoparticles induced by optical forces for SERS detection was reported by Patra *et al.* using evanescent waves<sup>[141]</sup> and by Fazio *et al.*, who exploited the prevalence of scattering forces over gradient forces to dynamically assemble gold nanorod aggregates.<sup>[142]</sup> Microtools for

SERS detection were reported by Vizsnyiczai *et al.*, who microfabricated probes with trapping positions spatially separated from the SERS detection area.<sup>[143]</sup>

One of the major advantages of the Raman scattering signal is that it is not affected by photobleaching.<sup>[144]</sup> This, in combination with extended trapping times, means that Raman tweezers can be employed as a label-free analysis method for monitoring cellular behavior on relatively long time scales. Chang *et al.* performed a real-time characterization of cellular response to oxidative stress using yeast cells.<sup>[145]</sup> Chen *et al.* monitored the lysis of *E. Coli* caused by factors from both outside and inside the cells.<sup>[146]</sup> In both cases, acquiring successive Raman spectra for several tens of minutes provided significant insight into the cellular responses to disruptive factors. Furthermore, Raman properties can be used as discriminating factor for cell sorting applications, as described in the Section 3.4.<sup>[147]</sup>

### 3.3. Microrheology measurements

The use of optical tweezers for microrheology measurements was pioneered by Mason and Weitz in the '90s<sup>[148]</sup> and has been discussed in detail elsewhere.<sup>[149–153]</sup> Optical tweezers can provide information about the viscoelastic properties of a fluid, given by the frequency-dependent ability of the fluid to store and dissipate energy. In comparison to other microrheological techniques, optical methods reduce the required sample volume from tens of milliliters to tens of microliters,<sup>[154]</sup> which facilitates the characterization of rare specimens.

Two different operating modes are commonly used:

- i)* Passive viscoelastic measurements: in this case, a micrometer-sized spherical particle is held in place by a stationary trap in a fluid at thermal equilibrium. The Brownian motion of the particle is recorded and used for calculating the trap stiffness and the shear complex modulus of the fluid starting from the generalized Langevin equation.<sup>[148]</sup>
- ii)* Active viscoelastic measurements: in this case, the trap holding the microparticle is displaced in a controlled manner and the bead motion is recorded and analyzed. Small-

amplitude oscillations over a wide range of frequencies, employing probes of different sizes, are used to characterize the linear viscoelastic properties, while large-amplitude strains of varying rates are used for investigating non-linear phenomena.<sup>[155]</sup> The phase shift between the trap displacement and the microbead motion can be correlated with the viscoelastic properties of the fluid.<sup>[150]</sup> Active measurements can help acquire information about stiff materials and can be used to investigate non-equilibrium behavior.

A schematic representation of different operating modes for viscoelastic measurements is shown in **Figure 4C**.

For accurate microrheology measurements, the precise calibration of optical tweezers is essential.<sup>[156–158]</sup> Additionally, the uniformity of the spherical particle sizes employed in the measurements has a significant effect on the accuracy. Bishop *et al.* used rotating laser-trapped particles for microrheology measurements and calculated that, for particles with a diameter in the range of 1.5 to 3.5  $\mu\text{m}$ , a 90 nm accuracy in particle size is required in order to have an error below 10 % in the calculated viscosity.<sup>[159]</sup>

Since the late '90s, optical tweezer-based microrheology measurements have been performed in living cells. Measuring the viscoelastic properties of cell membranes can be achieved using dual trap systems.<sup>[160]</sup> Briefly, after attaching two microbeads to opposite ends of a cell, one of the beads can be held in place by a stationary trap, while the other bead can be oscillated with the aid of a second trap. This approach was used by Sleep *et al.* in 1999 to investigate the viscoelasticity of human erythrocytes.<sup>[160]</sup> Yamada *et al.* used intrinsic lipid storage granules present in COS7 kidney epithelial cells for non-invasive microrheological measurements.<sup>[161]</sup> Endogenous subcellular bodies have since been employed in microrheological measurements in e.g. alveolar epithelial type II cells<sup>[162]</sup> and *S. pombe* cells.<sup>[163]</sup> An optical stretcher was employed for rheological measurements in a microfluidic chip by Lincoln *et al.* on two different fibroblast lines.<sup>[164]</sup> Laser-induced erythrocyte edge vibrations were employed for

probing the viscoelasticity of red blood cells.<sup>[165]</sup> Ayala *et al.* employed optical tweezers to determine the microrheological properties of fibroblasts, astrocytes and neurons.<sup>[166]</sup>

Nishizawa *et al.* recently reported a feedback-tracking method for microrheology in mouse fibroblasts and HeLa cells.<sup>[167]</sup>

Due to differences in measurement techniques and the inherent cell-to-cell variability, reported viscoelastic moduli of living cells differ by up to three orders of magnitude.<sup>[166]</sup>

However, this apparent inaccuracy of the reported results might be related to the influence of the measurement duration on the experimentally determined microrheological properties of living cells. Tassieri expressed his concern about the current use of optical tweezers for microrheological measurements in living cells, as there is a large mismatch between the time scales necessary for experimental data acquisition and the time scales of biological processes naturally taking place in living cells.<sup>[168]</sup>

### **3.4. Particle and cell sorting**

Typically, Fluorescence Activated Cell Sorting (FACS) is used as standard laboratory technique for sorting cells. However, FACS requires  $> 10^5$  cells to achieve a high yield, it relies on fluorescent labelling for sorting, and it can be relatively damaging to the cells due to the high hydrodynamic forces involved in the various processes.<sup>[169]</sup> This is why optical methods have been developed as alternatives with potential use for fragile or rare samples. Particle sorting, with the potential for use in cell sorting, is one of the earliest applications of optical manipulation methods. Optical methods for cell sorting and their effect on cell viability are discussed in <sup>[170]</sup>.

The use of optical manipulation for particle and cell sorting is of particular interest in combination with automated methods for the detection and selection of target cells. Different parameters can be employed for discriminating between the particles, such as size,<sup>[171,172]</sup> refractive index,<sup>[171]</sup> fluorescent properties,<sup>[173,174]</sup> elasticity<sup>[175]</sup> or Raman properties.<sup>[147]</sup> Most

often, optical particle sorting is performed in microfluidic systems with different outlets for the collection of different fractions of the sample. A microfluidic platform for cell sorting is schematically shown in **Figure 4D**.<sup>[176]</sup>

Optical trapping and manipulation of *Escherichia Coli* (*E. coli*) and *Saccharomyces cerevisiae* (yeast cells) for extended time periods was reported by Ashkin *et al.* in 1987 using infrared laser optical tweezers and trapping powers of 5-80 mW.<sup>[177]</sup> Single *E. coli* cells were trapped for up to 5 h to monitor reproduction, during which time the bacteria continued to divide and showed no sign of photodamage. The rod-shaped *E. coli* cells were also spatially oriented using two trapping beams. Yeast cells were manipulated with velocities of up to 100  $\mu\text{m}\cdot\text{s}^{-1}$ . The same year, Buican *et al.*<sup>[178]</sup> demonstrated the transport and separation of fluorescein isothiocyanate (FITC) stained polystyrene microspheres and fixed Chinese hamster ovary (CHO) cells. Two orthogonal beams were used for the propulsion and deflection of the particles and a pulse shape analyzer was employed for selecting target particles.

Grover *et al* argued in favor of using a counter-propagating dual-beam optical configuration for improving 3D cell manipulation and minimizing photostress due reduced laser power requirements.<sup>[172]</sup> They achieved transport of trapped cells over a distance of 1 mm, followed by optical sorting of erythrocytes from a mixed cell population.

Separation of silica and polymer particles based on size and refractive index differences was demonstrated by MacDonald *et al.*<sup>[171]</sup> They achieved a 96 % sorting efficiency and a throughput of 25 particles  $\text{s}^{-1}$ , higher than that of microfabricated-FACS systems.

Fluorescence-based sorting of microparticles<sup>[173]</sup> and cells<sup>[174]</sup> has been demonstrated in microfluidic chips, achieving recovery rates and purity rates higher than 90 % for a throughput of 5 cells  $\text{s}^{-1}$ .

Label-free sorting of cells with the aid of optical methods can also be performed based on Raman properties.<sup>[147]</sup> Two different types of lymphocytes (pre-B lymphoblasts from B cell lymphoma and T lymphoblasts from acute lymphoblastic leukemia) were identified with the aid of principal component analysis (PCA) based on their Raman properties. The acquisition of the Raman spectrum for a single cell can take up to 2 minutes, which makes Raman-based sorting extremely slow. However, no membrane integrity loss was observed even after prolonged optical manipulation.

### **3.5. Subcellular manipulation using optical methods**

Intracellular manipulation and monitoring has been attempted using a variety of techniques.<sup>[179]</sup> Optical methods allow high spatio-temporal resolution and have been employed for e.g. intracellular delivery of submicron entities or for direct manipulation of subcellular components. Current limitations to the subcellular applications of optical methods arise from the possibility of photo-induced damage and from the difficulties of optical manipulation in the cytoplasm.

#### *3.5.1. Laser-induced photoporation*

Laser-induced photoporation can facilitate local introduction of foreign material, such as DNA, biopharmaceuticals or nanoparticles (NPs), into target cells. This can be achieved either by directly using highly-focused laser beams for direct photoporation, or through indirect methods. Photoporation has been recently reviewed by Xiong *et al.*<sup>[180]</sup>

The first reported attempt at laser-induced photoporation for DNA transfection came in 1984 from Tsukakoshi *et al.*<sup>[181]</sup> By using 10 ns pulses from a Nd:YAG 355 nm laser, they generated 2-3  $\mu\text{m}$  pores in cell membranes that were able to self-heal in less than 0.5 s. This allowed DNA transfection of normal rat kidney cells with a success rate of 0.6 % when targeting the cytoplasm and 10.2 % with nuclear irradiation. In 2002, Tirlapur and König reported targeted transfection of the pEGFP-N<sub>1</sub> vector encoding the enhanced green

fluorescent protein (EGFP) gene with 100 % efficiency.<sup>[182]</sup> This was achieved by exposing Chinese hamster ovarian cells and rat-kangaroo kidney epithelial cells to 16 ms irradiation from a near infrared (800 nm) femtosecond pulsed 80 MHz Ti:sapphire laser with an average power of 50 – 100 mW. In 2005, Paterson *et al.* reported the transfection of Chinese hamster ovary cells with a plasmid expression vector containing an antibiotic resistance gene and the green fluorescent protein (GFP) gene by using low-power photoporation.<sup>[183]</sup> In this case, a violet laser diode (405 nm, 40 mW output) was used to induce photoporation in 40 ms exposure doses.

There are several different approaches for indirect photoporation of cell membranes with the aid of NPs, which have been developed in recent years as alternatives to direct photoporation in order to i) minimize the required laser power and thus the stress that the cells are exposed to and ii) increase the photoporation throughput. Reported indirect methods have employed plasmonic NPs or carbon nanostructures as sensitizers for photoporation.<sup>[180,184,185]</sup> A schematic of using gold nanoparticle-assisted photoporation for DNA transfection is shown in **Figure 4E**.

### 3.5.2. Cellular manipulation using nanoparticles

Intracellular delivery of NPs is a subject of interest in the research world as strategy for targeted drug delivery. Different endocytic routes and receptor-mediate pathways strategies for intracellular NP uptake have been recently reviewed by Yameen *et al.*<sup>[186]</sup>

A combination of optical tweezers and optical injection has been reported for targeted delivery of 100 nm gold NPs inside Chinese hamster ovarian cell nuclei.<sup>[184]</sup> A 1064 continuous wave laser source (25 mW at sample plane) was employed for optical tweezing, and a femtosecond-pulsed Ti:sapphire laser was employed for optical injection. The combination of optical methods allowed the intranuclear delivery of single gold NPs with a 10 % efficiency.

Dvir Yelin's group used plasmonic resonance of gold NPs for controlled cell damage and fusion.<sup>[187,188]</sup> The gold NPs were first modified with polyethylene glycol (PEG) and then further with antibodies that would allow them to specifically bind to the cell membrane of target cells. In their 2012 study, the group induced apoptosis in epidermoid carcinoma and Burkitt lymphoma B cells with the aid of membrane-bound gold NPs. The use of 16 pulses of 50 fs ( $35 \text{ mJ} \cdot \text{cm}^{-2}$ ) from a Ti:sapphire laser with the wavelength adjusted to 550 nm for plasmonic resonance with the gold NPs was sufficient to induce apoptosis in 90 % of the cells 23 h after exposure.<sup>[187]</sup> By using bispecific modification of gold NPs, Yelin's group reported controlled cell fusion of Burkitt lymphoma B and human monocyte-derived dendritic cells with an efficiency of about 7 % and no observable effect on cell viability after 24 h.<sup>[188]</sup>

#### **4. Measurements in complex media**

Optical trapping and manipulation in water has been successfully employed in the past decades for investigating a variety of biological systems. However, for a more accurate assessment of certain interactions taking place in biological systems, experiments benefit from being performed in real biological samples or, when this is not possible, in model systems that mimic their properties. The complexity of biological samples raises several challenges for optical trapping due to *i*) optical properties (e.g. refractive index, absorption, scattering properties) which alter light propagation and can influence the trapping forces; *ii*) microrheological properties (viscoelasticity); *iii*) interaction properties (e.g. hydrogen bonding between compounds present in the sample and polymeric microspheres or microrobots) and *iv*) sample to sample variability. The optical properties of human blood<sup>[189]</sup> and other various tissues<sup>[190,191]</sup> have been investigated since the use of laser surgery has become widespread. In addition to intracellular optical manipulation, discussed in Section 3.5, optical trapping experiments in complex biological samples have been reported in eye fluid,<sup>[192]</sup> cell culture media, seminal fluid and mucus. Furthermore, a few examples of *in vivo* optical trapping in

vertebrates were published recently. Examples of optical trapping applications in complex media are discussed in the following sections.

#### 4.1. Cell culture media

Cell culture media are relatively complex aqueous solutions that usually contain various quantities of salts, aminoacids, antibiotics and sugars and up to 10 % added serum. To ensure cell viability over prolonged periods of time, cell culture medium is far superior to water, and it can enable long-term trapping and manipulation experiments. Various types of cell culture media have been employed for optical trapping experiments.<sup>[193–195]</sup>

Pang *et al* demonstrated optical trapping of HIV-1 virions in culture fluid in a microfluidic chamber for measuring the virion diameters.<sup>[196]</sup> They employed a home-made optical tweezers instrument using a tapered amplifier diode laser at 830 nm. Jing *et al.* recently reported arbitrary patterning and characterization of human pluripotent stem cells in culture medium with the aid of photonic-crystal optical tweezers.<sup>[197]</sup>

#### 4.2. Seminal fluid

Sperm motility is an important quality factor for successful natural reproduction and artificial insemination. Optical tweezers have been used for assessing the swimming forces of individual spermatozoa from animal and human samples for the past three decades.

The first report of optical trapping of sperm came from Tadir *et al.* in 1989,<sup>[198]</sup> who investigated sperm motility in a mixture of HEPES buffer and Minimum Essential Media (MEM). Since then, several studies have used optical tweezers as a tool to study sperm motility, with a tendency to move towards biologically relevant media. Currently, most studies using human sperm are performed in HEPES-buffered modified human tubal fluid (mHTF) with 5 % serum substitute supplement (SSS). The effect of trap duration and laser power on sperm motility was investigated by Nascimento *et al.*<sup>[199]</sup> in Biggers, Whitten and Wittingham (BWW) medium supplemented with 1 mg·mL<sup>-1</sup> bovine serum albumin (BSA).

Two years later, the same group published a comparative study of sperm motility in primates<sup>[200]</sup>. The study was performed in BSA-supplemented BWW for primate semen samples, and in HEPES-buffered mHTF with 5 % SSS for human semen samples. In 2012, Hyun *et al.* investigated the effects of viscosity on human sperm motility.<sup>[201]</sup> The viscosity of the HEPES-buffered mHTF with 5 % SSS was varied between 1 and 15 cP, similar to native viscosities of the human male reproductive tract, by addition of methylcellulose (0.5 – 2 %). A 2017 study from Chow *et al.*<sup>[202]</sup> showed that exposure to red light increases the swimming force of spermatozoa.

The effect of optical tweezer manipulation on the viability of the cells is a factor that limits the applicability of the method for artificial insemination. However, optical tweezers provide a viable method of estimating swimming forces and thus help select high quality spermatozoa for artificial insemination.

### 4.3. Mucus

Mucus is a complex biological fluid that lubricates and protects moist mucosal surfaces and serves as a biobarrier against foreign particles, while allowing rapid passage of selected chemical compounds.<sup>[203]</sup> The biopolymeric mucus mesh has highly variable properties intermediate to a viscous liquid and an elastic solid. Its refractive index and viscosity are very different from water and vary based on species, individual and production site. This raises a significant challenge for optical trapping experiments in mucus.

Certain hydrogels (e.g. hydroxyethylcellulose, HEC, 140 kDa molecular mass) can be employed as model systems with relevant molecular weight and similar microrheological properties to mucus.<sup>[204]</sup> However, as shown in the work of Kirch *et al.*,<sup>[204]</sup> there are significant differences between the behavior of microbeads (4 – 5  $\mu\text{m}$  in diameter) in HEC gels as opposed to mucus. PEG-coated particles were shown to successfully penetrate HEC hydrogels, but were unable to migrate into horse pulmonary mucus samples. In addition,

mucus samples required the use of microbeads with higher refractive index (melamin resin beads,  $n = 1.68$ ) compared to HEC hydrogels, where polymethacrylate beads ( $n = 1.49$ ) were employed. Active tracking experiments were performed by using the signal of a waveform generator to induce a triangular oscillation pattern of the trap (**Figure 5**). In the HEC hydrogel, the microbeads were shown to follow the trap with a slight phase shift and a dampened amplitude. In mucus, the microbeads were unable to significantly react to the motion of the trap, thus proving that the confinement of particles in mucus raises a significant challenge for optical manipulation.

Weigand *et al.*<sup>[205]</sup> employed microbeads of different sizes to investigate the rheological properties of mucus from the *Chaetopterus* marine worm over different length scales. They tested different sizes of microbeads (2 – 10  $\mu\text{m}$  in diameter) in either pure or dilute mucus with 0.015 % added Tween 20. All beads were coated with Alexa Fluor 488 bovine serum albumin to reduce nonspecific binding to mucus and facilitate visualization of the beads. Their results showed that the size of the probe largely influences the behavior of the probe within the mucus mesh and allowed them to identify three different length scale regimes. This conclusion is important to keep in mind for designing optical trapping experiments in heterogenous environments.

### 4.3. *In vivo*

There are numerous reports of optical trapping *in vivo* in unicellular microorganisms such as bacteria,<sup>[206]</sup> amoebae,<sup>[207,208]</sup> or microalgae.<sup>[209]</sup> When it comes to multicellular organisms, and in particular to vertebrates, the main challenge for optical trapping *in vivo* is represented by the ability to focus the light at sufficient depth through living tissues.

Thin zebrafish larvae are optically transparent and thus particularly suited for *in vivo* optical studies. Johansen *et al.* demonstrated manipulation of injected nanoparticles and bacteria and endogenous erythrocytes and macrophages in living zebrafish larvae.<sup>[210]</sup> Manipulation of

otoliths with sizes up to 55 microns in living zebrafish larvae was reported by Favre-Bulle *et al.*<sup>[211]</sup>

*In vivo* optical manipulation of red blood cells was reported by Zhong *et al.* in mice.<sup>[212–214]</sup>

Optical tweezers were used to perform microsurgery to clear blocked capillaries in blood vessels present in mouse ears.<sup>[212]</sup> Trapping was possible using oil immersion objective up to a depth of  $\sim 40\ \mu\text{m}$ . The employed trapping laser power of 168 mW in the sample did not cause noticeable thermal damage. Optical trapping of erythrocytes using a water immersion objective was demonstrated up to a depth of  $\sim 60\ \mu\text{m}$  upon spherical aberration correction.<sup>[213]</sup> The papers from Zhong *et al.* also discuss the optical trap stiffness *in vivo*, the challenges posed by the variability of biological tissues and aberration compensation.

## 5. Strategies for improving optical trapping in biological samples

In order to overcome the challenges posed by optical trapping in biological samples, the two main options proposed are *i*) using adaptive light shaping and *ii*) tailoring the trapped object. The goal is to provide stable traps, while minimizing potential harmful side effects as the laser interacts with the trapped object or its surrounding environment.

### 5.1. Advanced beam-shaping

Beam-shaping is briefly discussed in Section 2.3. To achieve stable trapping in biological samples, one of the obvious options is to shape the laser light employed for optical manipulation. Beam-shaping has already become ubiquitous in optical trapping and manipulation experiments, where it is primarily used for simultaneously generating multiple traps, and with additional use of advanced laser modes for trapping.

In addition to generating multiple traps simultaneously, beam-shaping can ensure efficient use of the laser light power, which, combined with real-time reconfiguration of the beams, can help avoid the difficulties caused by the scattering and absorption properties of the samples. For example, *in situ* wavefront aberration correction using a method based on orthogonal

mode decomposition was shown to improve optical trapping in turbid media in a standard HOT geometry.<sup>[215]</sup>

Innovative trapping methods might also help advancements in manipulation in biological samples. For example, the use of shaped beams carrying orbital angular momentum was reviewed by Padgett and Bowman.<sup>[216]</sup> Other non-conventional approaches include trapping of gold NPs using femtosecond laser pulses, which induce nonlinear polarization,<sup>[217]</sup> the use of scattering microparticles for “enhanced trapping via structured scattering” (ENTRAPs)<sup>[218]</sup> or the potential use of the optical pulling force.<sup>[219]</sup> Optical “pulling” of particles in the Mie regime, instead of the usual “pushing”, was described by Chen *et al.* for beams composed of near-glancing plane-wave components through numerical simulations and analytical calculations using a Bessel beam as example.<sup>[219]</sup> Furthermore, optoelectronic tweezers<sup>[220,221]</sup> have also shown promise for cellular manipulation in cell culture media.<sup>[222,223]</sup>

## 5.2. Sculpting the object

Due to the basic principles of optical trapping methods, trapping targets have originally consisted mostly in microspheres of different sizes and refractive indices. The use of more complex light-controlled structures originates in the early 2000s<sup>[224]</sup> and has been growing tremendously in recent years,<sup>[225–228]</sup> helped by advancements in microfabrication techniques. Tailoring the microparticle properties can simultaneously improve its optical manipulation in biological samples and allow it to perform specific tasks. For these purposes, shape and topology optimization can be combined with surface modification of the microstructures.

### 5.2.1. Shape and topology optimization

Light-controllable microparticles can either have predefined shapes (e.g. microtools 3D-printed in commercial negative photoresists such as IP-L,<sup>[229]</sup> IP-G,<sup>[230]</sup> Femtobond 4B,<sup>[231]</sup> SCR-701<sup>[232]</sup>, NOA63<sup>[233]</sup> and SU-8<sup>[234,235]</sup> or fabricated in SiO<sub>2</sub> through a double liftoff photolithographic process<sup>[236]</sup>) or they can be based on light-responsive materials (e.g. light-

sensitive polymers<sup>[237]</sup> or liquid crystal elastomers<sup>[238]</sup>). Shape-changing microtools based on light-sensitive materials are responsive to light, but not amenable to optical trapping and manipulation, so they will not be further discussed here. Optical trapping and manipulation of microtools was reviewed by Palima and Glückstad in 2013.<sup>[239]</sup>

Examples of 3D-printed and optically-actuated microtools are shown in **Figure 6**. Through careful design, the microtools can be made to accomplish specific tasks. Precise optical micromanipulation of microfabricated tools was originally demonstrated by our group in both 2D<sup>[240]</sup> and 3D.<sup>[241,242]</sup> **Figure 6A** shows a simple microtool with four spherical “handles” for optical trapping and manipulation and a surface functionalized with fluorescent streptavidin.<sup>[235]</sup> **Figure 6B** shows a nut-and-screw assembly built by Köhler *et al* using 3D-printing followed by optical manipulation.<sup>[231]</sup> The screw is fixed on the surface and the loose nut is printed in a maze-like compartment that ensures the nut will not be lost during development. Through its four spherical “handles”, the nut is optically trapped and guided outside the maze-like compartment, where it is subsequently assembled with the fixed screw. Optically actuated surface scanning probes with different designs were reported by Phillips *et al*.<sup>[230,243]</sup> and one of the designs is shown in **Figure 6C**. The trap positions are displaced to scan a sample line-by-line and the spheres included in the probe are tracked in order to calculate the position of the tip, which allows a reconstruction of the sample topography. Our group has reported syringe-like microrobots with a hollow body.<sup>[229]</sup> These microrobots can be moved to a target site, loaded with cargo from their vicinity and then transported to a different site for unloading the cargo. Cargo loading/unloading is achieved by localized heating of a gold-coated segment of the microtool, which induces changes in the fluid flow around it. **Figure 6D** shows a sequence of images acquired during the loading of one such microrobot with a polystyrene microsphere. Other microrobot designs from our group include wave-guided optical waveguides<sup>[244]</sup> and disk-tools for localized heating in microfluidic

channels.<sup>[245]</sup> Kelemen's group employed SU-8-based microtools for indirect optical micromanipulation of single live cells.<sup>[246,247]</sup> **Figure 6E** shows one of these microtools used for cellular manipulation. The microtool was attached to a cell using streptavidin coating and used for indirect optical trapping with HOTs.

### 5.2.2. Surface modification

Surface modification of microtools employed in optical trapping experiments can improve their usefulness in biological samples in several different manners, as discussed below.

With regular optical tweezers, the trapping forces are in the piconewton range. By employing an antireflection coating on the particles, the trapping forces can be increased to the nanonewton level.<sup>[248–250]</sup> Higher forces imply more stable trapping and might provide the solution for precise manipulation in biological media.

Particle coating is ubiquitous in drug delivery, as it helps control the interaction between the drug carrier and its environment.<sup>[251]</sup> Findings from this field might prove highly relevant for enhancing the optical manipulation of microparticles in biological samples. For example, PEG is widely used for nano- and microparticle coating to reduce non-specific binding. PEGylation makes the particles “stealthy” in biological samples, as PEG chains induce a strong steric repulsion between the coated particle and surrounding molecules from the sample.<sup>[252]</sup>

Numerous other polymers, both synthetic (e.g. poly(acrylic acid), polyethers, Eudragit®) and natural (e.g. chitosan, cellulose, poly(L-lysine), have been employed in order to control the charge and the hydro/lipophilicity of particles and therefore their interaction with their environment.<sup>[252,253]</sup> Particles commonly used in optical trapping experiments include polystyrene microspheres and microfabricated SU-8 or poly(acrylate) based microtools. These have hydrophobic surfaces and can form hydrophobic interactions with molecules present in biological samples,<sup>[254]</sup> which can then lead to reduced optical control over the particles due to competing forces. The use of suitable polymeric coatings represents a viable option for

minimizing the microparticle-environment interactions, therefore improving optical manipulation in biological samples. For example, Weigand *et al.* employed BSA-coating to reduce interactions between microparticles and mucus for optical manipulation experiments.<sup>[205]</sup> On the other hand, when it is desirable to introduce stable interactions between a microtool and a certain biological sample, suitable surface functionalization can be employed. An example is the work of Aekbote *et al.*, who functionalized SU-8 microtools with streptavidin or IgG for cell attachment.<sup>[247]</sup> We have recently developed a method for functionalizing microtools fabricated using the IP-L 780 photoresist from Nanoscribe.<sup>[255]</sup> The use of surface modifications that can induce local changes in the environment is another option. Plasmon-enhanced optical heating of gold(-coated) micro- and nanostructures has been shown to induce localized temperature increase<sup>[245,256]</sup> even to the point of locally-melting phospholipid bilayers<sup>[257]</sup> or hydrogels<sup>[258]</sup>. Local heating leads to changes in the physicochemical properties of the sample (e.g. reduces viscosity) and could be an option for “softening” the sample in order to facilitate the manipulation of microtools inside complex biological environments. However, the effect of local heating on a specific biological sample should be evaluated for every application before employing it as a means to facilitate particle manipulation.

## 6. Conclusions and outlook

This review focused on the applications and perspectives of optical trapping techniques in biological samples. We provided a short description of the basic principles behind the optical trapping of isotropic and anisotropic particles. We then briefly discussed laser modes, beam-shaping and techniques for generating single and multiple traps. We gave an overview of the applications of optical trapping in aqueous solutions and discussed the applications in complex media. In the end, we suggested two strategies for improving optical trapping in biological samples.

Optical trapping methods have enabled tremendous advances in our understanding of living organisms, as emphasized by the 2018 Nobel Prize award in Physics to Arthur Ashkin "for the optical tweezers and their application to biological systems". This paper reviewed some of the most common areas of application of optical trapping methods in aqueous solutions, complex media and even in living organisms. Subjects such as single molecule studies, Raman analysis, microrheology or cell sorting have taken advantage of the precise manipulation possibilities provided by optical trapping.

To take full advantage of the potential of optical trapping methods, it is necessary to be able to perform the experiments in an environment as similar as possible to *in vivo* systems, either in real biological samples or in models with similar properties. Furthermore, recent years have shown that optical trapping needs not be employed only for studying biological systems, but can also trigger specific processes or enable certain functions in the sample. Through intelligent design of both the optical trapping system and the trapped object, microrobotic "surgeons" with the ability to perform specific functions in biological samples can be obtained. However, efficient optical control of such microtools in complex media is somewhat challenging due to the high variability of such samples and to inherent properties of the light-sample interactions. An interdisciplinary approach combining knowledge from photonics, engineering and surface chemistry might be able to provide the solution for precise actuation of microrobots in biological samples, which could then help shape the future of contemporary biomedical research.

### **Acknowledgements**

We acknowledge support from the Novo Nordisk Foundation (Grand Challenge Program; NNF16OC0021948) and VILLUM FONDEN (Research Grant 00022918).

We would like to acknowledge useful discussions with Dr. Andrew R. Bañas and Einstom Engay.

Received: ((will be filled in by the editorial staff))

Revised: ((will be filled in by the editorial staff))

Published online: ((will be filled in by the editorial staff))

## References

- [1] A. Ashkin, *Phys. Rev. Lett.* **1970**, *24*, 156.
- [2] A. Ashkin, J. M. Dziedzic, J. E. Bjorkholm, S. Chu, *Opt. Lett.* **1986**, *11*, 288.
- [3] H. Metcalf, *J. Opt. Soc. Am. B* **1989**, *6*, 2206.
- [4] O. Emile, F. Bardou, C. Salomon, P. Laurent, A. Nadir, A. Caliron, *Europhys. Lett.* **1992**, *20*, 687.
- [5] J. Glückstad, D. Palima, *Light Robotics : Structure-Mediated Nanobiophotonics*, Elsevier, **2017**.
- [6] A. Ashkin, *Proc. Natl. Acad. Sci.* **1997**, *94*, 4853.
- [7] K. C. Neuman, S. M. Block, *Rev. Sci. Instrum.* **2004**, *75*, 2787.
- [8] K. Dholakia, P. Reece, M. Gu, *Chem. Soc. Rev.* **2008**, *37*, 42.
- [9] J. R. Moffitt, Y. R. Chemla, S. B. Smith, C. Bustamante, *Annu. Rev. Biochem.* **2008**, *77*, 205.
- [10] J. E. Molloy, M. J. Padgett, *Contemp. Phys.* **2002**, *43*, 241.
- [11] R. W. Bowman, M. J. Padgett, *Reports Prog. Phys.* **2013**, *76*, 026401.
- [12] T. A. Nieminen, N. Du Preez-Wilkinson, A. B. Stilgoe, V. L. Y. Loke, A. A. M. Bui, H. Rubinsztein-Dunlop, *J. Quant. Spectrosc. Radiat. Transf.* **2014**, *146*, 59.
- [13] M. Daly, M. Sergides, S. Nic Chormaic, *Laser Photonics Rev.* **2015**, *9*, 309.
- [14] P. Polimeno, A. Magazzù, M. A. Iatì, F. Patti, R. Saija, C. D. Esposti Boschi, M. G. Donato, P. G. Gucciardi, P. H. Jones, G. Volpe, O. M. Maragò, *J. Quant. Spectrosc. Radiat. Transf.* **2018**, *218*, 131.
- [15] T. A. Nieminen, G. Knöner, N. R. Heckenberg, H. Rubinsztein-Dunlop, *Methods Cell Biol.* **2007**, *82*, 207.
- [16] Y. Harada, T. Asakura, *Opt. Commun.* **1996**, *124*, 529.
- [17] A. Gennerich, *Optical Tweezers*, Springer, **2017**.
- [18] G. Gouesbet, G. Gréhan, B. Maheu, *J. Opt.* **1985**, *16*, 83.
- [19] G. Gouesbet, G. Gréhan, *Generalized Lorenz-Mie Theories*, Springer, **2017**.
- [20] J. A. Lock, G. Gouesbet, *J. Quant. Spectrosc. Radiat. Transf.* **2009**, *110*, 800.
- [21] G. Gouesbet, G. Gréhan, B. Maheu, *Appl. Opt.* **1988**, *27*, 4874.
- [22] G. Gouesbet, G. Gréhan, *J. Mod. Opt.* **2000**, *47*, 821.
- [23] A. Rohrbach, *Phys. Rev. Lett.* **2005**, *95*, 168102.
- [24] P. J. Pauzauskie, A. Radenovic, E. Trepagnier, H. Shroff, P. Yang, J. Liphardt, *Nat. Mater.* **2006**, *5*, 97.
- [25] T. Yu, F.-C. Cheong, C.-H. Sow, *Nanotechnology* **2004**, *15*, 1732.
- [26] M. E. J. Friese, T. A. Nieminen, N. R. Heckenberg, H. Rubinsztein-Dunlop, *Nature* **1998**, *394*, 348.
- [27] H. Zhang, K.-K. Liu, *J. R. Soc. Interface* **2008**, *5*, 671.
- [28] T. A. Nieminen, V. L. Y. Loke, A. B. Stilgoe, G. Knöner, A. M. Brańczyk, N. R. Heckenberg, H. Rubinsztein-Dunlop, *J. Opt. A Pure Appl. Opt.* **2007**, *9*, S196.
- [29] T. A. Nieminen, V. L. Y. Loke, A. B. Stilgoe, N. R. Heckenberg, H. Rubinsztein-Dunlop, *J. Mod. Opt.* **2011**, *58*, 528.
- [30] E. Higurashi, H. Ukita, H. Tanaka, O. Ohguchi, *Appl. Phys. Lett.* **1994**, *64*, 2209.
- [31] T. A. Nieminen, H. Rubinsztein-Dunlop, N. R. Heckenberg, *J. Quant. Spectrosc. Radiat. Transf.* **2001**, *70*, 627.
- [32] S. H. Simpson, S. Hanna, *J. Opt. Soc. Am. A* **2007**, *24*, 430.

- [33] C. Selhuber-Unkel, I. Zins, O. Schubert, C. Sönnichsen, L. B. Oddershede, *Nano Lett.* **2008**, *8*, 2998.
- [34] S. H. Simpson, S. Hanna, *Opt. Express* **2011**, *19*, 16526.
- [35] K. Kim, Y. Park, *Nat. Commun.* **2017**, *8*, 15340.
- [36] Y. Cao, A. B. Stilgoe, L. Chen, T. A. Nieminen, H. Rubinsztein-Dunlop, *Opt. Express* **2012**, *20*, 12987.
- [37] S. Parkin, G. Knöner, W. Singer, T. A. Nieminen, N. R. Heckenberg, H. Rubinsztein-Dunlop, *Methods Cell Biol.* **2007**, *82*, 525.
- [38] S. H. Simpson, S. Hanna, *Phys. Rev. E* **2010**, *82*, 031141.
- [39] O. M. Maragò, P. H. Jones, P. G. Gucciardi, G. Volpe, A. C. Ferrari, *Nat. Nanotechnol.* **2013**, *8*, 807.
- [40] S. H. Simpson, *J. Quant. Spectrosc. Radiat. Transf.* **2014**, *146*, 81.
- [41] H. Kogelnik, T. Li, *Appl. Opt.* **1966**, *5*, 1550.
- [42] K. Dholakia, T. Čižmár, *Nat. Photonics* **2011**, *5*, 335.
- [43] M. Woerdemann, C. Alpmann, M. Esseling, C. Denz, *Laser Photon. Rev.* **2013**, *7*, 839.
- [44] C.-W. Qiu, D. Palima, A. Novitsky, D. Gao, W. Ding, S. V. Zhukovsky, J. Glückstad, *Nanophotonics* **2014**, *3*, 181.
- [45] H. Rubinsztein-Dunlop, A. Forbes, M. V Berry, M. R. Dennis, D. L. Andrews, M. Mansuripur, C. Denz, C. Alpmann, P. Banzer, T. Bauer, E. Karimi, L. Marrucci, M. Padgett, M. Ritsch-Marte, N. M. Litchinitser, N. P. Bigelow, C. Rosales-Guzmán, A. Belmonte, J. P. Torres, T. W. Neely, M. Baker, R. Gordon, A. B. Stilgoe, J. Romero, A. G. White, R. Fickler, A. E. Willner, G. Xie, B. McMorran, A. M. Weiner, *J. Opt.* **2017**, *19*, 013001.
- [46] F. M. Dickey, *Laser Beam Shaping: Theory and Techniques*, CRC Press, **2014**.
- [47] G. Behrman, M. Duignan, *Appl. Opt.* **1997**, *36*, 4666.
- [48] G. Knöner, S. Parkin, T. A. Nieminen, V. L. Y. Loke, N. R. Heckenberg, H. Rubinsztein-Dunlop, *Opt. Express* **2007**, *15*, 5521.
- [49] J. H. McLeod, *J. Opt. Soc. Am.* **1954**, *44*, 592.
- [50] C. Maurer, A. Jesacher, S. Bernet, M. Ritsch-Marte, *Laser Photonics Rev.* **2011**, *5*, 81.
- [51] K. Dholakia, T. Čižmár, *Nat. Photonics* **2011**, *5*, 335.
- [52] A. S. Bezryadina, D. C. Preece, J. C. Chen, Z. Chen, *Light Sci. Appl.* **2016**, *5*, e16158.
- [53] B. Hadad, S. Froim, H. Nagar, T. Admon, Y. Eliezer, Y. Roichman, A. Bahabad, *Optica* **2018**, *5*, 551.
- [54] V. R. Daria, D. Z. Palima, J. Glückstad, *Opt. Express* **2011**, *19*, 476.
- [55] R. L. Eriksen, P. C. Mogenssen, J. Glückstad, *Opt. Lett.* **2002**, *27*, 267.
- [56] R. Lynge Eriksen, V. Ricardo Daria, J. Glückstad, *Opt. Express* **2002**, *10*, 597.
- [57] J. Glückstad, *Opt. Commun.* **1996**, *130*, 225.
- [58] J. Glückstad, D. Palima, *Generalized Phase Contrast : Applications in Optics and Photonics*, Springer, **2009**.
- [59] P. J. Rodrigo, I. R. Perch-Nielsen, J. Glückstad, *Opt. Express* **2006**, *14*, 5812.
- [60] A. Bañas, J. Glückstad, *Opt. Commun.* **2017**, *392*, 190.
- [61] A. Ashkin, *Biophys. J.* **1992**, *61*, 569.
- [62] M.-D. Wei, W.-L. Shiao, Y.-T. Lin, *Opt. Commun.* **2005**, *248*, 7.
- [63] P. Genevet, J. Dellinger, R. Blanchard, A. She, M. Petit, B. Cluzel, M. A. Kats, F. de Fornel, F. Capasso, *Opt. Express* **2013**, *21*, 10295.
- [64] J. Arlt, M. J. Padgett, *Opt. Lett.* **2000**, *25*, 191.
- [65] D. McGloin, G. C. Spalding, H. Melville, W. Sibbett, K. Dholakia, *Opt. Commun.* **2003**, *225*, 215.
- [66] C. Alpmann, M. Esseling, P. Rose, C. Denz, *Appl. Phys. Lett.* **2012**, *100*, 111101.
- [67] M. M. Burns, J. M. Fournier, J. A. Golovchenko, *Science*. **1990**, *249*, 749.

- [68] H. Misawa, K. Sasaki, M. Koshioka, N. Kitamura, H. Masuhara, *Appl. Phys. Lett.* **1992**, *60*, 310.
- [69] K. Visscher, G. J. Brakenhoff, J. J. Krol, *Cytometry* **1993**, *14*, 105.
- [70] D. Palima, T. B. Lindballe, M. V Kristensen, S. Tauro, H. Stapelfeldt, S. R. Keiding, J. Glückstad, *J. Opt.* **2011**, *13*, 044013.
- [71] E. R. Lyons, G. J. Sonek, *Appl. Phys. Lett.* **1995**, *66*, 1584.
- [72] K. Taguchi, K. Atsuta, T. Nakata, M. Ikeda, *Opt. Commun.* **2000**, *176*, 43.
- [73] E. Sidick, S. D. Collins, A. Knoesen, *Appl. Opt.* **1997**, *36*, 6423.
- [74] S. Ebert, K. Travis, B. Lincoln, J. Guck, *Opt. Express* **2007**, *15*, 15493.
- [75] V. G. Shvedov, A. S. Desyatnikov, A. V. Rode, W. Krolikowski, Y. S. Kivshar, *Opt. Express* **2009**, *17*, 5743.
- [76] T. Čižmár, O. Brzobohatý, K. Dholakia, P. Zemánek, *Laser Phys. Lett.* **2011**, *8*, 50.
- [77] S. Zwick, T. Haist, Y. Miyamoto, L. He, M. Warber, A. Hermerschmidt, W. Osten, *J. Opt. A Pure Appl. Opt.* **2009**, *11*, 034011.
- [78] M. Pitzek, R. Steiger, G. Thalhammer, S. Bernet, M. Ritsch-Marte, *Opt. Express* **2009**, *17*, 19414.
- [79] P. J. Rodrigo, V. R. Daria, J. Glückstad, *Opt. Lett.* **2004**, *29*, 2270.
- [80] P. J. Rodrigo, V. R. Daria, J. Glückstad, *Opt. Express* **2004**, *12*, 1417.
- [81] P. John Rodrigo, I. R. Perch-Nielsen, C. Amadeo Alonzo, J. Glückstad, *Opt. Express* **2006**, *14*, 13107.
- [82] P. J. Rodrigo, V. R. Daria, J. Glückstad, *Appl. Phys. Lett.* **2005**, *86*, 074103.
- [83] D. G. Grier, *Nature* **2003**, *424*, 810.
- [84] E. R. Dufresne, G. C. Spalding, M. T. Dearing, S. a. Sheets, D. G. Grier, *Rev. Sci. Instrum.* **2001**, *72*, 1810.
- [85] J. A. Rodrigo, A. M. Caravaca-Aguirre, T. Alieva, G. Cristóbal, M. L. Calvo, *Opt. Express* **2011**, *19*, 5232.
- [86] B. Sun, Y. Roichman, D. G. Grier, *Opt. Express* **2008**, *16*, 15765.
- [87] J. Bergman, O. Osunbayo, M. Vershinin, *Sci. Rep.* **2016**, *5*, 18085.
- [88] P. Korda, G. C. Spalding, E. R. Dufresne, D. G. Grier, *Rev. Sci. Instrum.* **2002**, *73*, 1956.
- [89] R. W. Bowman, G. M. Gibson, A. Linnenberger, D. B. Phillips, J. A. Grieve, D. M. Carberry, S. Serati, M. J. Miles, M. J. Padgett, *Comput. Phys. Commun.* **2014**, *185*, 268.
- [90] M. Padgett, R. Di Leonardo, *Lab Chip* **2011**, *11*, 1196.
- [91] K. Sasaki, M. Koshioka, H. Misawa, N. Kitamura, H. Masuhara, *Appl. Phys. Lett.* **1992**, *60*, 807.
- [92] H. He, N. R. Heckenberg, H. Rubinsztein-Dunlop, *J. Mod. Opt.* **1995**, *42*, 217.
- [93] K. T. Gahagan, G. A. Swartzlander, *Opt. Lett.* **1996**, *21*, 827.
- [94] M. P. MacDonald, L. Paterson, W. Sibbett, K. Dholakia, P. E. Bryant, *Opt. Lett.* **2001**, *26*, 863.
- [95] V. R. Daria, P. J. Rodrigo, J. Glückstad, *Appl. Phys. Lett.* **2004**, *84*, 323.
- [96] M. L. Juan, M. Righini, R. Quidant, *Nat. Photonics* **2011**, *5*, 349.
- [97] A. A. E. Saleh, J. A. Dionne, *Nano Lett.* **2012**, *12*, 5581.
- [98] A. Lehmuskero, P. Johansson, H. Rubinsztein-Dunlop, L. Tong, M. Käll, *ACS Nano* **2015**, *9*, 3453.
- [99] A. Lehmuskero, Y. Li, P. Johansson, M. Käll, *Opt. Express* **2014**, *22*, 4349.
- [100] R. Quidant, C. Girard, *Laser Photonics Rev.* **2008**, *2*, 47.
- [101] T. Shoji, Y. Tsuboi, *J. Phys. Chem. Lett.* **2014**, *5*, 2957.
- [102] J. E. Baker, R. P. Badman, M. D. Wang, *Wiley Interdiscip. Rev. Nanomedicine Nanobiotechnology* **2018**, *10*, e1477.

- [103] A. S. Urban, S. Carretero-Palacios, A. A. Lutich, T. Lohmüller, J. Feldmann, F. Jäckel, *Nanoscale* **2014**, *6*, 4458.
- [104] M. Righini, A. S. Zelenina, C. Girard, R. Quidant, *Nat. Phys.* **2007**, *3*, 477.
- [105] K. Okamoto, S. Kawata, *Phys. Rev. Lett.* **1999**, *83*, 4534.
- [106] M. L. Juan, R. Gordon, Y. Pang, F. Eftekhari, R. Quidant, *Nat. Phys.* **2009**, *5*, 915.
- [107] O. J. F. Martin, C. Girard, *Appl. Phys. Lett.* **1997**, *70*, 705.
- [108] L. Novotny, R. X. Bian, X. S. Xie, *Phys. Rev. Lett.* **1997**, *79*, 645.
- [109] Y. Pang, R. Gordon, *Nano Lett.* **2012**, *12*, 402.
- [110] A. Kotnala, R. Gordon, *Nano Lett.* **2014**, *14*, 853.
- [111] A. A. Al Balushi, R. Gordon, *ACS Photonics* **2014**, *1*, 389.
- [112] Y. Tanaka, S. Kaneda, K. Sasaki, *Nano Lett.* **2013**, *13*, 2146.
- [113] A. N. Grigorenko, N. W. Roberts, M. R. Dickinson, Y. Zhang, *Nat. Photonics* **2008**, *2*, 365.
- [114] M. Righini, P. Ghenuche, S. Cherukulappurath, V. Myroshnychenko, F. J. García de Abajo, R. Quidant, *Nano Lett.* **2009**, *9*, 3387.
- [115] J.-H. Kang, K. Kim, H.-S. Ee, Y.-H. Lee, T.-Y. Yoon, M.-K. Seo, H.-G. Park, *Nat. Commun.* **2011**, *2*, 582.
- [116] W. Zhang, L. Huang, C. Santschi, O. J. F. Martin, *Nano Lett.* **2010**, *10*, 1006.
- [117] B. J. Roxworthy, K. D. Ko, A. Kumar, K. H. Fung, E. K. C. Chow, G. L. Liu, N. X. Fang, K. C. Toussaint, *Nano Lett.* **2012**, *12*, 796.
- [118] Y. Tsuboi, T. Shoji, N. Kitamura, M. Takase, K. Murakoshi, Y. Mizumoto, H. Ishihara, *J. Phys. Chem. Lett.* **2010**, *1*, 2327.
- [119] F. M. Fazal, S. M. Block, *Nat. Photonics* **2011**, *5*, 318.
- [120] M. J. Villangca, D. ; Casey, J. Glückstad, *Biophys. Rev.* **2015**, *7*, 379.
- [121] P. Rodríguez-Sevilla, L. Labrador-Páez, D. Jaque, P. Haro-González, *J. Mater. Chem. B* **2017**, *5*, 9085.
- [122] A. L. Forget, S. C. Kowalczykowski, *Nature* **2012**, *482*, 423.
- [123] M. J. Comstock, T. Ha, Y. R. Chemla, *Nat. Methods* **2011**, *8*, 335.
- [124] A. N. Gupta, A. Vincent, K. Neupane, H. Yu, F. Wang, M. T. Woodside, *Nat. Phys.* **2011**, *7*, 631.
- [125] T. Ha, *Nat. Methods* **2014**, *11*, 1015.
- [126] C. Veigel, C. F. Schmidt, *Nat. Rev. Mol. Cell Biol.* **2011**, *12*, 163.
- [127] E. A. Abbondanzieri, W. J. Greenleaf, J. W. Shaevitz, R. Landick, S. M. Block, *Nature* **2005**, *438*, 460.
- [128] E. Dieterich, J. Camunas-Soler, M. Ribezzi-Crivellari, U. Seifert, F. Ritort, *Nat. Phys.* **2015**, *11*, 971.
- [129] C. S. S. R. Kumar, *Raman Spectroscopy for Nanomaterials Characterization*, Springer, **2012**.
- [130] M. Y. Wu, D. X. Ling, L. Ling, W. Li, Y. Q. Li, *Sci. Rep.* **2017**, *7*, 42930.
- [131] L. Rkiouak, M. J. Tang, J. C. J. Camp, J. McGregor, I. M. Watson, R. A. Cox, M. Kalberer, A. D. Ward, F. D. Pope, *Phys. Chem. Chem. Phys.* **2014**, *16*, 11426.
- [132] Z. Gong, Y. Le Pan, G. Videen, C. Wang, *Anal. Chim. Acta* **2018**, *1020*, 86.
- [133] K. Svoboda, S. M. Block, *Opt. Lett.* **1994**, *19*, 930.
- [134] P. M. Hansen, V. K. Bhatia, N. Harrit, L. Oddershede, *Nano Lett.* **2005**, *5*, 1937.
- [135] L. Bosanac, T. Aabo, P. M. Bendix, L. B. Oddershede, *Nano Lett.* **2008**, *8*, 1486.
- [136] E. C. Le Ru, P. G. Etchegoin, *Principles of Surface-Enhanced Raman Spectroscopy : And Related Plasmonic Effects*, Elsevier, **2009**.
- [137] F. Svedberg, Z. Li, H. Xu, M. Käll, *Nano Lett.* **2006**, *6*, 2639.
- [138] Y. Tanaka, H. Yoshikawa, T. Itoh, M. Ishikawa, *J. Phys. Chem. C* **2009**, *113*, 11856.
- [139] G. McNay, F. T. Docherty, D. Graham, W. E. Smith, P. Jordan, M. Padgett, J. Leach,

- G. Sinclair, P. B. Monaghan, J. M. Cooper, *Angew. Chemie Int. Ed.* **2004**, *43*, 2512.
- [140] Š. Bálint, M. P. Kreuzer, S. Rao, G. Badenes, P. Miškovský, D. Petrov, *J. Phys. Chem. C* **2009**, *113*, 17724.
- [141] P. P. Patra, R. Chikkaraddy, R. P. N. Tripathi, A. Dasgupta, G. V. P. Kumar, *Nat. Commun.* **2014**, *5*, 4357.
- [142] B. Fazio, C. D'Andrea, A. Foti, E. Messina, A. Irrera, M. G. Donato, V. Villari, N. Micali, O. M. Maragò, P. G. Gucciardi, *Sci. Rep.* **2016**, *6*, 26952.
- [143] G. Vizsnyiczai, T. Lestyán, J. Joniova, B. L. Aekbote, A. Strejčková, P. Ormos, P. Miskovsky, L. Kelemen, G. Bánó, *Langmuir* **2015**, *31*, 10087.
- [144] J. W. Chan, *J. Biophotonics* **2013**, *6*, 36.
- [145] W.-T. Chang, H.-L. Lin, H.-C. Chen, Y.-M. Wu, W.-J. Chen, Y.-T. Lee, I. Liao, *J. Raman Spectrosc.* **2009**, *40*, 1194.
- [146] D. Chen, L. Shelenkova, Y. Li, C. R. Kempf, A. Sabelnikov, *Anal. Chem.* **2009**, *81*, 3227.
- [147] A. Y. Lau, L. P. Lee, J. W. Chan, *Lab Chip* **2008**, *8*, 1116.
- [148] T. G. Mason, D. A. Weitz, *Phys. Rev. Lett.* **1995**, *74*, 1250.
- [149] V. Tuchin, *Handbook of Photonics for Biomedical Science.*, Taylor & Francis, **2010**.
- [150] R. R. Brau, J. M. Ferrer, H. Lee, C. E. Castro, B. K. Tam, P. B. Tarsa, P. Matsudaira, M. C. Boyce, R. D. Kamm, M. J. Lang, *J. Opt. A Pure Appl. Opt.* **2007**, *9*, S103.
- [151] J. M. Tassieri, M. Evans, R.M.L., Warren, R.L., Bailey, N.J., and Cooper, *New J. Phys.* **2012**, *14*, 115032.
- [152] A. Yao, M. Tassieri, M. Padgett, J. Cooper, *Lab Chip* **2009**, *9*, 2568.
- [153] L. J. Gibson, S. Zhang, A. B. Stilgoe, T. A. Nieminen, H. Rubinsztein-Dunlop, *Phys. Rev. E* **2017**, *95*, 042608.
- [154] M. Tassieri, F. Del Giudice, E. J. Robertson, N. Jain, B. Fries, R. Wilson, A. Glidle, F. Greco, P. A. Netti, P. L. Maffettone, T. Bicanic, J. M. Cooper, *Sci. Rep.* **2015**, *5*, 8831.
- [155] K. Regan, S. Ricketts, R. Robertson-Anderson, *Polymers (Basel)*. **2016**, *8*, 336.
- [156] M. Fischer, K. Berg-Sørensen, *J. Opt. A Pure Appl. Opt.* **2007**, *9*, S239.
- [157] M. Andersson, F. Czerwinski, L. B. Oddershede, *J. Opt.* **2011**, *13*, 044020.
- [158] J. R. Staunton, B. Blehm, A. Devine, K. Tanner, *Opt. Express* **2017**, *25*, 1746.
- [159] A. I. Bishop, T. A. Nieminen, N. R. Heckenberg, H. Rubinsztein-Dunlop, *Phys. Rev. Lett.* **2004**, *92*, 14.
- [160] J. Sleep, D. Wilson, R. Simmons, W. Gratzer, *Biophys. J.* **1999**, *77*, 3085.
- [161] S. Yamada, D. Wirtz, S. C. Kuo, *Biophys. J.* **2000**, *78*, 1736.
- [162] M.-T. Wei, A. Zaorski, H. C. Yalcin, J. Wang, M. Hallow, S. N. Ghadiali, A. Chiou, H. D. Ou-Yang, *Opt. Express* **2008**, *16*, 8594.
- [163] J. Mas, A. C. Richardson, S. N. S. Reihani, L. B. Oddershede, K. Berg-Sørensen, *Phys. Biol.* **2013**, *10*, 046006.
- [164] B. Lincoln, F. Wottawah, S. Schinkinger, S. Ebert, J. Guck, *Methods Cell Biol.* **2007**, *83*, 397.
- [165] E. V. Lyubin, *J. Biomed. Opt.* **2012**, *17*, 101510.
- [166] Y. A. Ayala, B. Pontes, D. S. Ether, L. B. Pires, G. R. Araujo, S. Frases, L. F. Romão, M. Farina, V. Moura-Neto, N. B. Viana, H. Moysés Nussenzveig, *BMC Biophys.* **2016**, *9*, 1.
- [167] K. Nishizawa, M. Bremerich, H. Ayade, C. F. Schmidt, T. Ariga, D. Mizuno, *Sci. Adv.* **2017**, *3*, e1700318.
- [168] M. Tassieri, *Soft Matter* **2015**, *11*, 5792.
- [169] M. M. Wang, E. Tu, D. E. Raymond, J. M. Yang, H. Zhang, N. Hagen, B. Dees, E. M. Mercer, A. H. Forster, I. Kariv, P. J. Marchand, W. F. Butler, *Nat. Biotechnol.* **2005**, *23*, 83.

- [170] D. Palima, T. Aabo, A. Bañas, J. Glückstad, in *Photonics Biomed. Photonics, Spectrosc. Microsc.* (Ed.: D.L. Andrews), Wiley, **2015**, pp. 197–237.
- [171] M. P. MacDonald, G. C. Spalding, K. Dholakia, *Nature* **2003**, *426*, 421.
- [172] S. C. Grover, A. G. Skirtach, R. C. Gauthier, C. P. Grover, *J. Biomed. Opt.* **2001**, *6*, 14.
- [173] R. W. Applegate Jr., J. Squier, T. Vestad, J. Oakey, D. W. M. Marr, P. Bado, M. A. Dugan, A. A. Said, *Lab Chip* **2006**, *6*, 422.
- [174] X. Wang, S. Chen, M. Kong, Z. Wang, K. D. Costa, R. A. Li, D. Sun, *Lab Chip* **2011**, *11*, 3656.
- [175] J. Guck, R. Ananthakrishnan, C. C. Cunningham, J. Käs, *J. Phys. Condens. Matter* **2002**, *14*, 4843.
- [176] A. Bañas, D. Palima, M. Villangca, J. Glückstad, in *Proc. SPIE*, **2016**.
- [177] A. Ashkin, J. M. Dziedzic, T. Yamane, *Nature* **1987**, *330*, 769.
- [178] T. N. Buican, M. J. Smyth, H. A. Crissman, G. C. Salzman, C. C. Stewart, J. C. Martin, *Appl. Opt.* **1987**, *26*, 5311.
- [179] J. Liu, J. Wen, Z. Zhang, H. Liu, Y. Sun, *Microsystems Nanoeng.* **2015**, *1*, 15020.
- [180] R. Xiong, S. K. Samal, J. Demeester, A. G. Skirtach, S. C. De Smedt, K. Braeckmans, *Adv. Phys. X* **2016**, *1*, 596.
- [181] M. Tsukakoshi, S. Kurata, Y. Nomiya, Y. Ikawa, T. Kasuya, *Appl. Phys. B Photophysics Laser Chem.* **1984**, *35*, 135.
- [182] U. K. Tirlapur, K. König, *Nature* **2002**, *418*, 290.
- [183] L. Paterson, B. Agate, M. Comrie, R. Ferguson, T. K. Lake, J. E. Morris, A. E. Carruthers, C. T. A. Brown, W. Sibbett, P. E. Bryant, F. Gunn-Moore, A. C. Riches, K. Dholakia, *Opt. Express* **2005**, *13*, 595.
- [184] C. McDougall, D. J. Stevenson, C. T. A. Brown, F. Gunn-Moore, K. Dholakia, *J. Biophotonics* **2009**, *2*, 736.
- [185] M. Waleed, S.-U. Hwang, J.-D. Kim, I. Shabbir, S.-M. Shin, Y.-G. Lee, *Biomed. Opt. Express* **2013**, *4*, 1533.
- [186] B. Yameen, W. Il Choi, C. Vilos, A. Swami, J. Shi, O. C. Farokhzad, *J. Control. Release* **2014**, *190*, 485.
- [187] L. Minai, D. Yeheskely-Hayon, L. Golan, G. Bisker, E. J. Dann, D. Yelin, *Small* **2012**, *8*, 1732.
- [188] D. Yeheskely-Hayon, L. Minai, L. Golan, E. J. Dann, D. Yelin, *Small* **2013**, *9*, 3771.
- [189] A. Roggan, M. Friebel, K. Dörschel, A. Hahn, G. Müller, *J. Biomed. Opt.* **1999**, *4*, 36.
- [190] W. F. Cheong, S. A. Prahl, A. J. Welch, *IEEE J. Quantum Electron.* **1990**, *26*, 2166.
- [191] S. L. Jacques, *Phys. Med. Biol.* **2013**, *58*, R37.
- [192] S. Zhang, L. J. Gibson, A. B. Stilgoe, I. A. Favre-Bulle, T. A. Nieminen, H. Rubinsztein-Dunlop, *Optica* **2017**, *4*, 1103.
- [193] D. J. Stevenson, T. K. Lake, B. Agate, V. Gárcés-Chávez, K. Dholakia, F. Gunn-Moore, *Opt. Express* **2006**, *14*, 9786.
- [194] R. W. Steubing, S. Cheng, W. H. Wright, Y. Numajiri, M. W. Berns, *Cytometry* **1991**, *12*, 505.
- [195] B. J. Roxworthy, M. T. Johnston, F. T. Lee-Montiel, R. H. Ewoldt, P. I. Imoukhuede, K. C. Toussaint, *PLoS One* **2014**, *9*, e93929.
- [196] Y. Pang, H. Song, J. H. Kim, X. Hou, W. Cheng, *Nat. Nanotechnol.* **2014**, *9*, 624.
- [197] P. Jing, Y. Liu, E. G. Keeler, N. M. Cruz, B. S. Freedman, L. Y. Lin, *Biomed. Opt. Express* **2018**, *9*, 771.
- [198] Y. Tadir, W. H. Wright, O. Vafa, T. Ord, R. H. Asch, M. W. Berns, *Fertil. Steril.* **1989**, *52*, 870.
- [199] J. M. Nascimento, J. L. Nascimento, E. L. Botvinick, L. Z. Shi, B. Durrant, M. W. Berns, *J. Biomed. Opt.* **2006**, *11*, 044001.

- [200] J. M. Nascimento, L. Z. Shi, S. Meyers, P. Gagneux, N. M. Loskutoff, E. L. Botvinick, M. W. Berns, *J. R. Soc. Interface* **2008**, *5*, 297.
- [201] N. Hyun, C. Chandsawangbhuwana, Q. Zhu, L. Z. Shi, C. Yang-Wong, M. W. Berns, *J. Biomed. Opt.* **2012**, *17*, 025005.
- [202] K. W. Chow, D. Preece, M. W. Berns, *Biomed. Opt. Express* **2017**, *8*, 4200.
- [203] S. K. Lai, Y. Y. Wang, D. Wirtz, J. Hanes, *Adv. Drug Deliv. Rev.* **2009**, *61*, 86.
- [204] J. Kirch, A. Schneider, B. Abou, A. Hopf, U. F. Schaefer, M. Schneider, C. Schall, C. Wagner, C.-M. Lehr, *Proc. Natl. Acad. Sci.* **2012**, *109*, 18355.
- [205] W. J. Weigand, A. Messmore, J. Tu, A. Morales-Sanz, D. L. Blair, D. D. Deheyn, J. S. Urbach, R. M. Robertson-Anderson, *PLoS One* **2017**, *12*, e0176732.
- [206] A. Ashkin, J. Dziedzic, *Science*. **1987**, *235*, 1517.
- [207] A. Ashkin, K. Schütze, J. M. Dziedzic, U. Euteneuer, M. Schliwa, *Nature* **1990**, *348*, 346.
- [208] B. H. Blehm, T. A. Schroer, K. M. Trybus, Y. R. Chemla, P. R. Selvin, *Proc. Natl. Acad. Sci. United States Am.* **2013**, *110*, 33871.
- [209] H. Wu, J. V. Volponi, A. E. Oliver, A. N. Parikh, B. A. Simmons, S. Singh, *Proc. Natl. Acad. Sci. U. S. A.* **2011**, *108*, 3809.
- [210] P. L. Johansen, F. Fenaroli, L. Evensen, G. Griffiths, G. Koster, *Nat. Commun.* **2016**, *7*, 10974.
- [211] I. A. Favre-Bulle, A. B. Stilgoe, H. Rubinsztein-Dunlop, E. K. Scott, *Nat. Commun.* **2017**, *8*, 630.
- [212] M.-C. Zhong, X.-B. Wei, J.-H. Zhou, Z.-Q. Wang, Y.-M. Li, *Nat. Commun.* **2013**, *4*, 1768.
- [213] M.-C. Zhong, L. Gong, J.-H. Zhou, Z.-Q. Wang, Y.-M. Li, *Opt. Lett.* **2013**, *38*, 5134.
- [214] M.-C. Zhong, Z.-Q. Wang, Y.-M. Li, *Appl. Opt.* **2017**, *56*, 1972.
- [215] T. Čížmár, M. Mazilu, K. Dholakia, *Nat. Photonics* **2010**, *4*, 388.
- [216] M. Padgett, R. Bowman, *Nat. Photonics* **2011**, *5*, 343.
- [217] Y. Jiang, T. Narushima, H. Okamoto, *Nat. Phys.* **2010**, *6*, 1005.
- [218] M. A. Taylor, M. Waleed, A. B. Stilgoe, H. Rubinsztein-Dunlop, W. P. Bowen, *Nat. Photonics* **2015**, *9*, 669.
- [219] J. Chen, J. Ng, Z. Lin, C. T. Chan, *Nat. Photonics* **2011**, *5*, 531.
- [220] P. Y. Chiou, A. T. Ohta, M. C. Wu, *Nature* **2005**, *436*, 370.
- [221] M. C. Wu, *Nat. Photonics* **2011**, *5*, 322.
- [222] Y. Yang, Y. Mao, K.-S. Shin, C. O. Chui, P.-Y. Chiou, *Sci. Rep.* **2016**, *6*, 22630.
- [223] H. Hsu, A. T. Ohta, P.-Y. Chiou, A. Jamshidi, S. L. Neale, M. C. Wu, *Lab Chip* **2010**, *10*, 165.
- [224] P. Galajda, P. Ormos, *Appl. Phys. Lett.* **2001**, *78*, 249.
- [225] G. A. Swartzlander, T. J. Peterson, A. B. Artusio-Glimpse, A. D. Raisanen, *Nat. Photonics* **2010**, *5*, 48.
- [226] J. Glückstad, *Nat. Photonics* **2011**, *5*, 7.
- [227] H. Zeng, P. Wasylczyk, D. S. Wiersma, A. Priimagi, *Adv. Mater.* **2018**, *30*, 1703554.
- [228] S. Nocentini, C. Parmeggiani, D. Martella, D. S. Wiersma, *Adv. Opt. Mater.* **2018**, *6*, 1800207.
- [229] M. J. Villangca, D. Palima, A. R. Bañas, J. Glückstad, *Light Sci. Appl.* **2016**, *5*, e16148.
- [230] D. B. Phillips, M. J. Padgett, S. Hanna, Y.-L. D. Ho, D. M. Carberry, M. J. Miles, S. H. Simpson, *Nat. Photonics* **2014**, *8*, 400.
- [231] J. Köhler, S. Isabelle Ksouri, C. Esen, A. Ostendorf, *Microsystems Nanoeng.* **2017**, *3*, 16083.
- [232] S. Maruo, A. Takaura, Y. Saito, *Opt. Express* **2009**, *17*, 18525.
- [233] T. Asavei, V. L. Y. Loke, M. Barbieri, T. A. Nieminen, N. R. Heckenberg, H.

- Rubinsztein-Dunlop, *New J. Phys.* **2009**, *11*, 093021.
- [234] G. Vizsnyiczai, G. Frangipane, C. Maggi, F. Saglimbeni, S. Bianchi, R. Di Leonardo, *Nat. Commun.* **2017**, *8*, 15974.
- [235] B. Lakshmanrao, J. Jacak, G. J. Schütz, E. Csányi, Z. Szegletes, P. Ormos, L. Kelemen, *Eur. Polym. J.* **2012**, *48*, 1745.
- [236] M. E. J. Friese, H. Rubinsztein-Dunlop, J. Gold, P. Hagberg, D. Hanstorp, *Appl. Phys. Lett.* **2001**, *78*, 547.
- [237] S. Fusco, M. S. Sakar, S. Kennedy, C. Peters, R. Bottani, F. Starsich, A. Mao, G. A. Sotiriou, S. Pané, S. E. Pratsinis, D. Mooney, B. J. Nelson, *Adv. Mater.* **2014**, *26*, 952.
- [238] K. Fuchi, T. H. Ware, P. R. Buskohl, G. W. Reich, R. A. Vaia, T. J. White, J. J. Joo, *Soft Matter* **2015**, *11*, 7288.
- [239] D. ; Palima, J. Glückstad, *Laser Photon. Rev.* **2013**, *7*, 478.
- [240] P. J. Rodrigo, L. Kelemen, C. A. Alonzo, I. R. Perch-Nielsen, J. S. Dam, P. Ormos, J. Glückstad, *Opt. Express* **2007**, *15*, 9009.
- [241] P. J. Rodrigo, L. Kelemen, D. Palima, C. A. Alonzo, P. Ormos, J. Glückstad, *Opt. Express* **2009**, *17*, 6578.
- [242] P. J. Rodrigo, L. Gammelgaard, P. Bøggild, I. Perch-Nielsen, J. Glückstad, *Opt. Express* **2005**, *13*, 6899.
- [243] D. B. Phillips, G. M. Gibson, R. Bowman, M. J. Padgett, S. Hanna, D. M. Carberry, M. J. Miles, S. H. Simpson, *Opt. Express* **2012**, *20*, 29679.
- [244] D. Palima, A. R. Bañas, G. Vizsnyiczai, L. Kelemen, P. Ormos, J. Glückstad, *Opt. Express* **2012**, *20*, 2004.
- [245] E. Engay, A.-I. Bunea, M. Chouliara, A. Bañas, J. Glückstad, *Opt. Lett.* **2018**, *43*, 3870.
- [246] G. Vizsnyiczai, B. L. Aekbote, A. Buzás, I. Grexa, P. Ormos, L. Kelemen, in (Eds.: K. Dholakia, G.C. Spalding), *International Society For Optics And Photonics*, **2016**, p. 992216.
- [247] B. L. Aekbote, T. Fekete, J. Jacak, G. Vizsnyiczai, P. Ormos, L. Kelemen, *Biomed. Opt. Express* **2016**, *7*, 45.
- [248] Y. Hu, T. A. Nieminen, N. R. Heckenberg, H. Rubinsztein-Dunlop, *J. Appl. Phys.* **2008**, *103*, 093119.
- [249] A. Jannasch, A. F. Demirörs, P. D. J. Van Oostrum, A. Van Blaaderen, E. Schäffer, *Nat. Photonics* **2012**, *6*, 469.
- [250] S. E. S. Spesyvtseva, K. Dholakia, *ACS Photonics* **2016**, *3*, 719.
- [251] A. Verma, F. Stellacci, *Small* **2010**, *6*, 12.
- [252] N. Hadjesfandiari, A. Parambath, in *Eng. Biomater. Drug Deliv. Syst.*, Woodhead Publishing, **2018**, pp. 345–361.
- [253] K. Babiuch, M. Gottschaldt, O. Werz, U. S. Schubert, *RSC Adv.* **2012**, *2*, 10427.
- [254] A. Faghijnejad, H. Zeng, *Soft Matter* **2012**, *8*, 2746.
- [255] A.-I. Bunea, M. H. Jakobsen, E. Engay, A. R. Bañas, J. Glückstad, *Micro Nano Eng.* **2018**, DOI 10.1016/J.MNE.2018.12.004.
- [256] R. Rodríguez-Oliveros, J. A. Sánchez-Gil, *Opt. Express* **2012**, *20*, 621.
- [257] J. T. Jørgensen, K. Norregaard, P. Tian, P. M. Bendix, A. Kjaer, L. B. Oddershede, *Sci. Rep.* **2016**, *6*, 30076.
- [258] S. Palagi, A. G. Mark, K. Melde, T. Qiu, H. Zeng, C. Parmeggiani, D. Martella, D. S. Wiersma, P. Fischer, in *Int. Conf. Manip. Autom. Robot. Small Scales, MARSS*, **2017**, pp. 1–5.

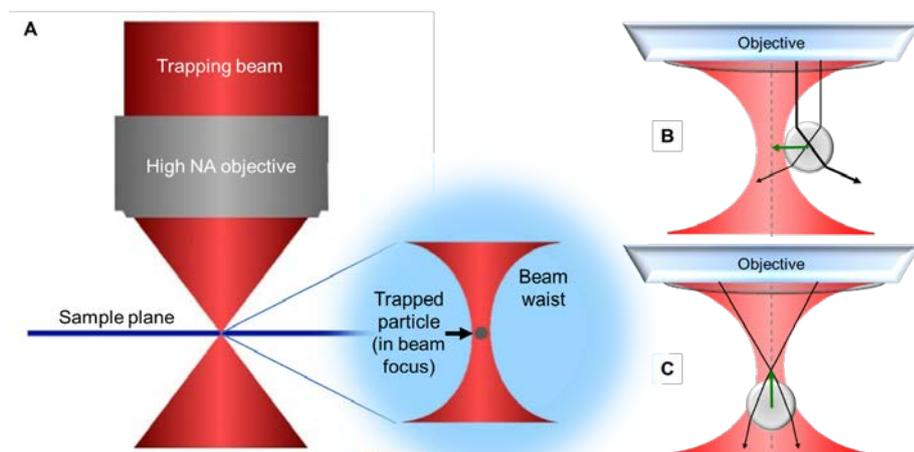


**Figure 1:** Illustration showing the basic principles of optical trapping for a simple gradient force optical tweezer. (A) A trapping beam is focused with the aid of a high numerical aperture objective into the sample plane and a particle can then be trapped in the focal point of the beam due to the large intensity gradients created. (B, C) Trapping in the Mie regime for transparent particles with xy offset (B) or with z-offset (C) from the beam focus. The refraction of light through the particle (black lines) results in gradient forces (shown as green arrow) attracting the particle towards the beam's focal point, where the light intensity is the highest.

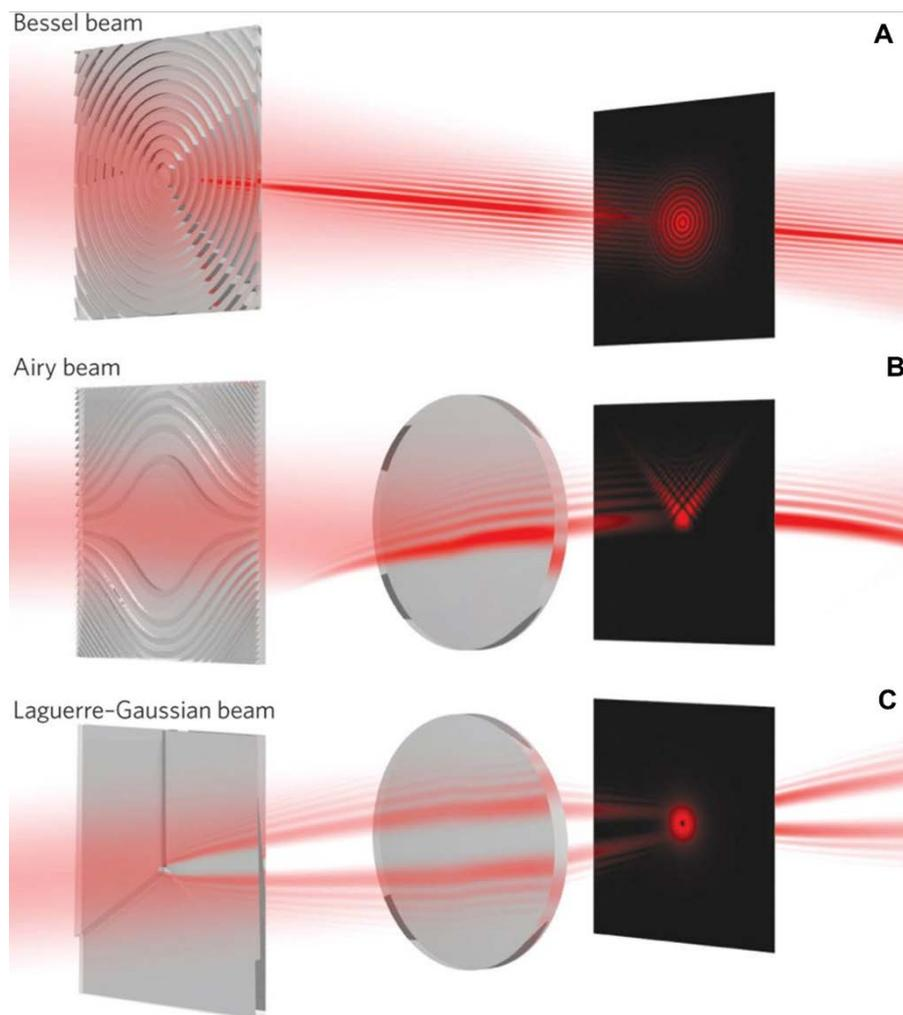


**Figure 2:** Examples of elaborate laser modes generated by diffractive elements. (A) A 'non-diffracting' zero-order Bessel beam generated by a diffractive axicon, offering an axially extended high-intensity central core that has the ability to reconstruct itself after passing an obstacle. (B) A 'non-diffracting' Airy beam generated by a diffractive cubic phase mask in the back focal plane of a convex lens. This mode propagates along a parabolic trajectory, in contrast with a Bessel beam. (C) Optical vortex with a topological charge of  $l = 3$  generated by a helical phase mask and focused by a lens. The on-axis phase singularity leads to the characteristic annular intensity. The helical wavefronts of such fields indicate that they possess orbital angular momentum that can be transferred to matter. Figure and caption adapted from Dholakia and Čižmár.<sup>[51]</sup>

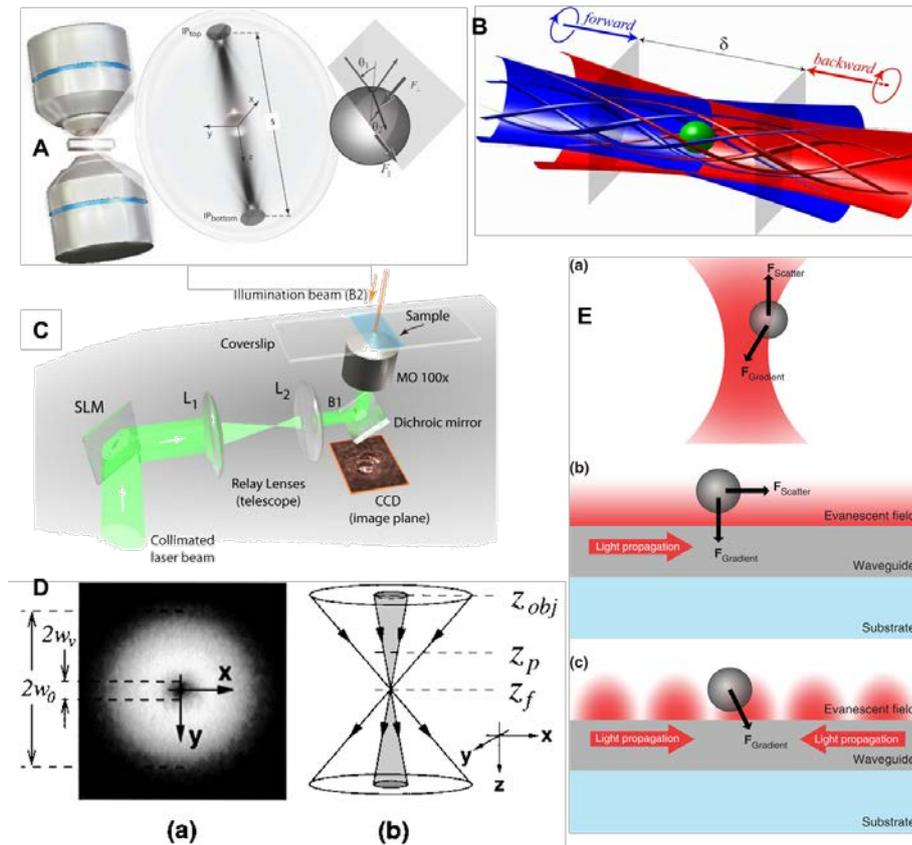


**Figure 3:** Examples of optical trapping methods. (A) Counter-propagating beam optical trap generated using Generalized Phase Contrast. (B) Optical trap with two counter-propagating co-rotating vortex beams. (C) Holographic optical tweezers setup relying on a spatial light modulator (SLM). Magneto-optical trap based on three mutually orthogonal, counter-propagating pairs of laser beams. (D) Vortex beam with a dark central core for dark optical trapping. (E) (a) Standard optical tweezers. (b) Trapping a dielectric bead near the surface of a nanophotonic waveguide. The optical gradient force toward the surface is due to the evanescent field decay. (c) Establishing a stationary standing wave in the waveguide eliminates the scattering force. Reproduced with permission from: A-<sup>[70]</sup>, B-<sup>[75]</sup>, C-<sup>[85]</sup>, D-<sup>[93]</sup>, E-<sup>[102]</sup>.

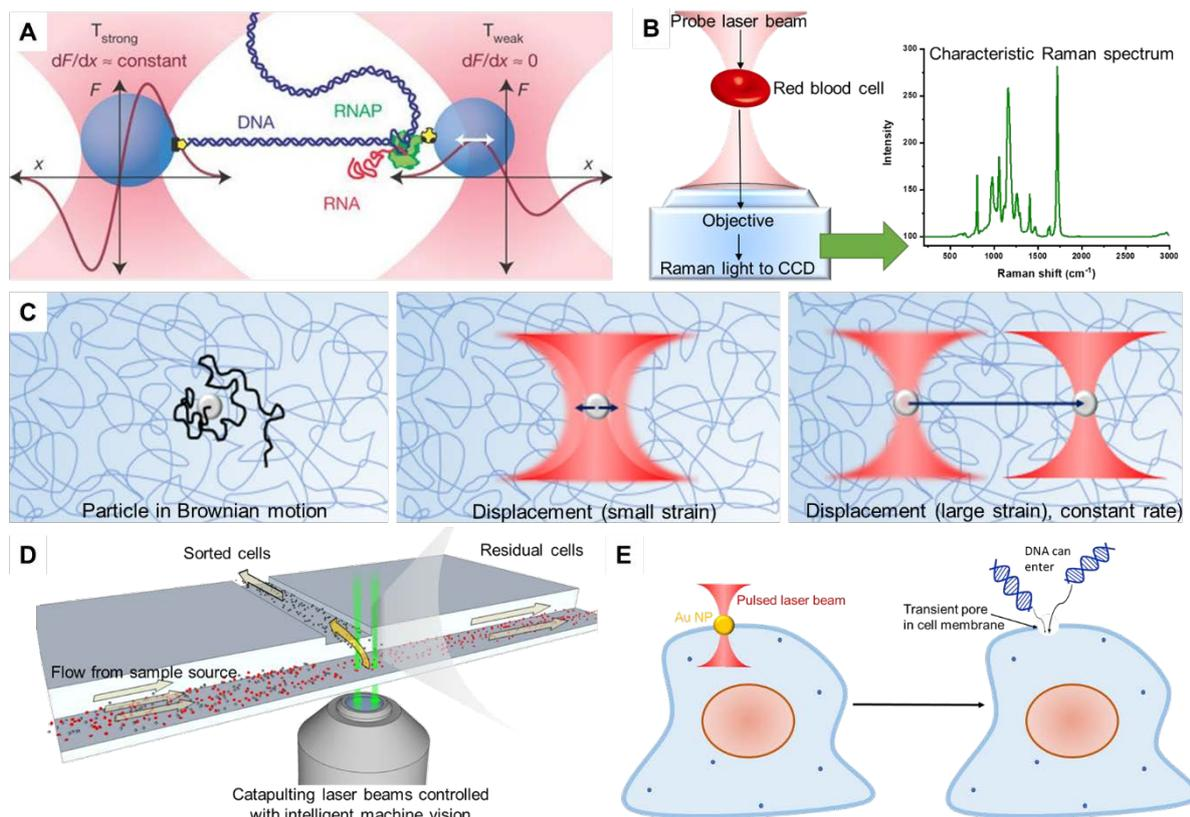


**Figure 4:** Schematic representations of optical trapping applications for biological samples. (A) Dumbbell geometry for monitoring transcriptional elongation by single molecules of *Escherichia coli* RNAP with Ångström-level resolution (reproduced with permission from [127]) (B) Raman tweezers measurements on a red blood cell. (C) Microrheology measurements: left – tracking of particle in Brownian motion for determining steady-state properties; middle: applying a small oscillatory strain for determining the linear viscoelasticity; right: applying a large constant rate strain for determining the nonlinear viscoelasticity. (D) Platform for cell sorting using catapulting laser beams (figure adapted from [176]). (E) Gold nanoparticle-assisted photoporation creates a transient pore in the cell membrane and enables DNA transfection.

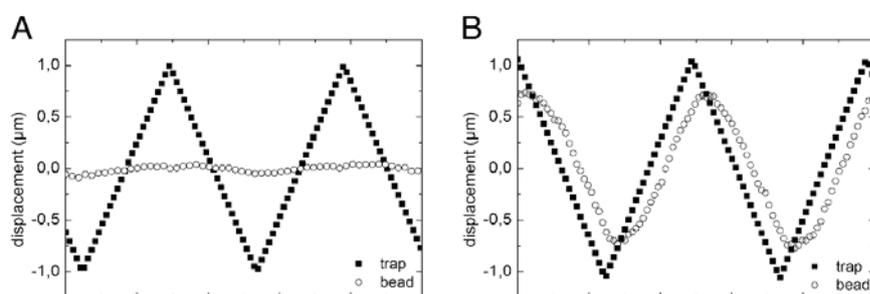


**Figure 5:** Active microrheology measurements in (A) horse pulmonary mucus and (B) hydroxyethylcellulose (HEC) hydrogels. In mucus, the bead shows no significant response to the trap displacement, while in HEC, the bead follows the trap with a slight phase shift and a dampened amplitude (B). Figure reproduced from [204].

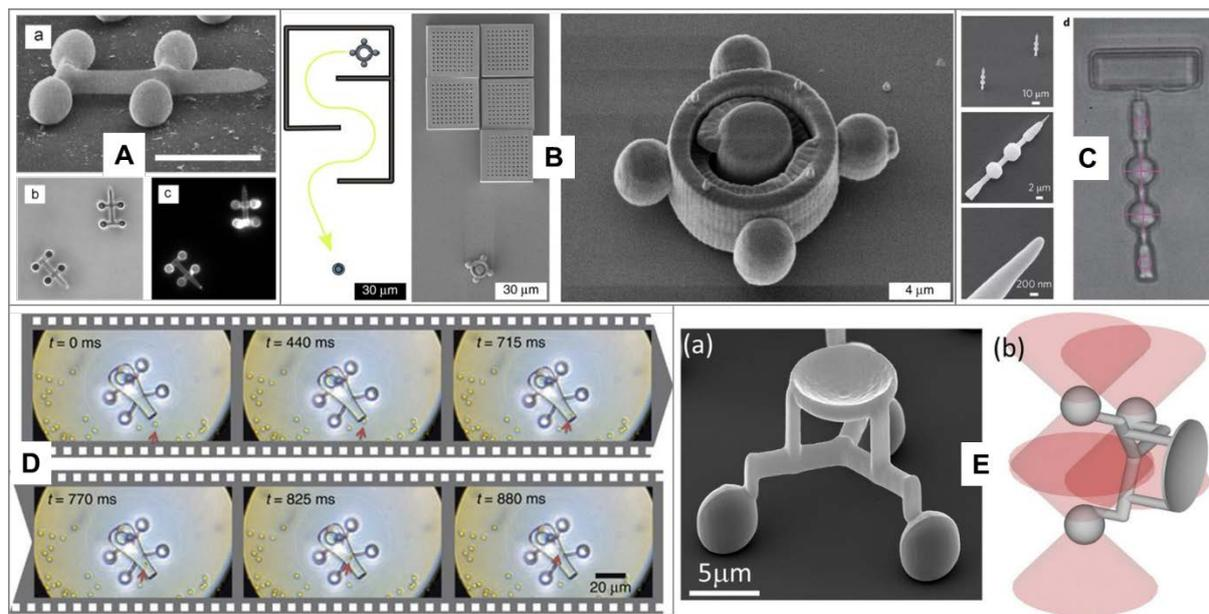


**Figure 6:** Examples of 3D-printed microtools with spherical trapping handles amenable to optical manipulation and serving different purposes. (A) Microtools functionalized with fluorescent streptavidin (a) SEM, (b) bright field and (c) fluorescence microscopy images. (B) Nut printed in a maze compartment structure is moved to a fixed screw and assembled on it through optical manipulation. (C) Surface scanning probe. Circles indicate the location of the optical traps and crosses mark the tracked regions of the probe. (D) Hollow-body syringe-like microrobot being loaded with microparticles by means of thermoplasmonic-induced convection. (E) Streptavidin-coated microtool for indirect live cell manipulation – SEM image and schematic of optical trapping. (Reproduced with permission from: A-<sup>[235]</sup>, B-<sup>[231]</sup>, C-<sup>[230]</sup>, D-<sup>[229]</sup> and E-<sup>[246]</sup>).



**Ada-Ioana Bunea** has a PhD in Micro- and Nanotechnology from the Technical University of Denmark (DTU) and is currently leading a project on BioBots, Light Robotics microtools applied in biological samples. Originally trained as a chemist at the University of Bucharest, in Romania, her background is highly interdisciplinary, combining fabrication, surface modification and characterization techniques.

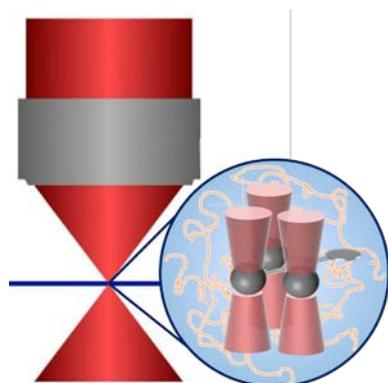


**Jesper Glückstad** established Programmable Phase Optics in Denmark two decades ago. He obtained his PhD from the Niels Bohr Institute in 1994 and his Doctor of Science from DTU in 2004. He invented GPC and its holographic extensions, pioneered Light Robotics, and published two books on these inventions. He is recipient of several awards including Ib Henriksen's «Scientist of the Year» prize in 2005. He co-founded OptoRobotix ApS in Silicon Valley in 2011 and is a Fellow of both OSA and SPIE.

## Graphical Abstract

Optical trapping is a tremendously useful tool for investigating biological systems. Overcoming the challenges of trapping in complex media is the next step for further enhancing the usefulness of optical trapping methods. A synergistic exploitation of advanced beam-shaping, microfabrication techniques and surface modification could be the key for developing a toolbox of optically-controlled microrobotic “surgeons” with various biomedical applications.

ToC figure



ToC keyword: Optical trapping